UNIVERSITÀ DEGLI STUDI DI PALERMO

Dottorato di ricerca in Oncologia e Chirurgia Sperimentali
Dipartimento di Discipline Chirurgiche Oncologiche e Stomatologiche (Di.Chir.On.S.)
International PhD course in "Experimental Oncology and Surgery" (Cycle XXIX)
University of Palermo and Universiteit Antwerpen

In Vitro and in Vivo investigation on stem cells isolated from pulp and gingival tissues from periodontally compromised teeth.

Doctoral Dissertation of:
Rodolfo Mauceri

Supervisors:
Prof. Silvio Abati
Prof. Michele Mignogna

Tutor Unipa:
Prof. Giuseppe Pizzo

Tutor UAntwerpen:
Prof. Christian Rolfo
Prof. Olivier Vanderveken

The Chair of the Doctoral Program:
Prof. Giuseppina Campisi

Years 2014/2016 - Cycle XXIX

UNIVERSITÀ DEGLI STUDI DI PALERMO

Dipartimento di Discipline Chirurgiche, Oncologiche e Stomatologiche (Di.Chir.On.S.)

Universiteit Antwerpen

Faculty of Medicine and Health Sciences

International joint PhD program

University of Palermo (Italy) and Universiteit Antwerpen (Belgium)

Title of the thesis:

In Vitro and in Vivo investigation on stem cells isolated from pulp and gingival tissues from periodontally compromised teeth.

Doctoral Dissertation of:
Dr. Rodolfo Mauceri

Supervisors:
Prof. Silvio Abati
Prof. Michele Mignogna

Tutor Unipa:
Prof. Giuseppe Pizzo

Tutor UAntwerpen:
Prof. Christian Rolfo
Prof. Olivier Vanderveken

The Chair of the Doctoral Program:
Prof. Giuseppina Campisi

Thesis for the Degree of Doctor in Medical Sciences (In de medische wetenschappen) at the Universiteit Antwerpen to be defended by Rodolfo Mauceri.

Thesis for the Degree of Doctor in Experimental Oncology and Surgery – (University of Palermo).

Years 2014/2016 - Cycle XXIX

INDEX

Abstract

Tissue engineering (TE) and regenerative medicine are interdisciplinary fields that provide new regenerated tissues by the development of biological substitutes that restore, maintain and or improve tissue function.

Dental pulp stem cells (DPSCs) and gingival mesenchymal stem cells (GMSCS) are a valuable source of stem cells for bone tissues regeneration.

The main objective of the present study is to evaluate the ability of DPSCs and GMSCs harvested from periodontally-affected teeth to produce *in vitro* and *in vivo* new mineralized bone tissue, in comparison to healthy teeth.

Weefsel engineering (TE) en regeneratieve geneeskunde zijn interdisciplinaire vakgebieden die samen zorgen voor weefselregeneratie door de ontwikkeling van biologische alternatieven die de weefselfunctie herstellen, onderhouden en verbeteren.

Dentale pulpa stamcellen (DPSCs) en gingivale mesenchymale stamcellen (GMSCs) zijn waardevolle bronnen voor stamcellen voor botweefsel regeneratie.

Het hoofddoel van de huidige studie is om de capaciteit na te gaan van deze DPSCs en GMSCs, geoogst uit periodontaal aangetaste tanden, om in vitro en in vivo nieuw gemineraliseerd botweefsel te produceren, in vergelijking met gezonde tanden.

Summary (Informative Abstract)

Dental pulp stem cells (DPSCs) and gingival mesenchymal stem cell (GMSCs) represent an alternative source of mesenchymal stem cells, their features make them ideal for bone tissue engineering. In this study, we verified the ability of DPSCs and GMSCs harvested from periodontally compromised teeth to produce *in vitro* and *in vivo* new mineralized bone tissue, in comparison to healthy teeth.

Initially, we isolate DPSCs and GMSCs from dental pulp and gingiva harvested from patients suffering of severe periodontitis (Test group) and from healthy patients (Control group). To characterize DPSCs and GMSCs colony-forming assay and cytofluorimetric and mRNA real time quantification analysis were performed. The effects of pro-inflammatory cytokines on MSC cell proliferation and differentiation potential were investigated. Furthermore, we investigated the capability of DPSCs and GMSCs to colonize Poly-L-lactic Acid (PLLA) scaffolds, produced by mean of Thermally Induced Phase Separation technique (TIPS). Finally, we investigate the capability of DPSCs and GMSCs from both studied groups to induce bone formation *in vivo*.

Our findings provide evidence that tissue (both pulp and gingiva) from periodontally-compromise teeth can be used as source of MSCs with intact stem properties and increased differentiation potential. Pro-inflammatory cytokines activate a cytoskeleton remodeling by recruiting heat shock proteins (HSPs) including HSP90, HSPA9, thioredoxin-1and actin-depolymerizing factors (ADFs) as profilin-1, cofilin-1 and vinculin that probably mediated the advantage acquisition in inflamed environment. Moreover, the DPSCs and GMSCs have been shown the capability to colonize successfully the PLLA scaffolds, but, in the animal study group, we did not observe new bone formation. Indeed, new in vivo studies are ongoing: PLLA scaffolds with DPSCs or GMSCs were implanted, in order to provide a more stable osteoinductive and osteoconductive structural support.

Dentale pulpa stamcellen (DPSCs) en gingivale mesenchymale stamcellen (GMSCs) vertegenwoordigen een alternatieve bron voor mesenchymale stamcellen. De eigenschappen van deze celtypes maken hun tot ideale kandidaten voor botweefsel engineering. In deze studie gingen we na of DPSCs en GMSCs, geoogst uit periodontaal aangetaste tanden, in staat zijn om in vitro en in vivo nieuw gemineraliseerd botweefsel te genereren, in vergelijking met gezonde tanden.

Eerst isoleerden we DPSCs en GMSCs uit de dentale pulpa en gingiva van patiënten die leden aan ernstige periodontitis (test groep) en gezonde patiënten (controle groep). Om deze DPSCs en GMSCs te karakteriseren voerden we de kolonie-vormende assay, cytofluorimetrische en mRNA real-time

kwantificatie analyses uit. Vervolgens werden de effecten van pro-inflammatoire cytokines op de proliferatie en differentiatie van MSC cellen onderzocht. Verder onderzochten we de capaciteit van DPSCs en GMSCs om Poly-L melkzuur (PLLA) substraat te koloniseren, dat geproduceerd werd door de thermaal geïnduceerde faseschеidingstechniek (TIPS). Tenslotte onderzochten we de capaciteit van DPSCs en GMSCs van beide studiegroepen om botvorming te induceren in vivo.

Onze resultaten bewezen dat weefsels (zowel uit de pulpa als uit de gingiva) uit periodontaal aangetaste tanden gebruikt kunnen worden als een bron voor MSCs met intacte stamceleigenschappen en verhoogd differentiatiepotentieel. Pro-inflammatoire cytokines activeren een cytoskelet herschikking door hitteschok eiwitten (HSPs) te rekruteren, zoals HSP90, HSPA9, thioredoxin-1 en actine-depolymeriserende factoren (ADF) zoals profilin-1, cofilin-1 en vinculin die waarschijnlijk de voordelen van een inflammatoire omgeving regelen. Bovendien vertoonden DPSCs en GMSCs de capaciteit om met succes PLLA substraten te koloniseren, maar in de dierlijke studiegroep hebben we geen nieuwe botformatie geobserveerd. Nieuwe in vivo studies worden momenteel uitgevoerd: PLLA substraten die DPSCs of GMSCs bevatten, werden geïmplanteerd om meer stabiele osteoïnductieve en osteoconductieve structurele steun te bieden.

CHAPTER 1

Background, Rationale and Objectives

1.1 Restoring missing teeth and bone resorption

Missing teeth and supporting oral tissues have traditionally been replaced with dentures or bridges permitting restoration of chewing function, speech, and aesthetics[1,2].

In the last decades, the use of dental implants has been increasingly applied to replace the missing teeth; indeed, today, dental implants are defined as the first-choice treatment modality for replacing missing teeth[3,4].

Historically, osseo-integration was firstly described by Branemark 1977 and is defined as the direct structural and functional connection between living bone and implant surface[5,6]. The achievement and the maintenance of osseo-integration is linked with implant stability, essential for successful long-terms results[7,8].

Implant stability is obtained mechanically during the insertion of the fixture in the jawbones; subsequently, the bone remodelling around the implants create a direct structural and functional connection between living bone and implant surface[6,8,9].

A sufficient bone volume to achieve primary implant stability is needed to place dental implants; however, bone resorption is a pathophysiological process induced by many mechanisms.

Primarly, the main cause of jawbone resorption is related to tooth loss, other factors that may influence the bone anatomy are trauma, surgery or congenital malformation. In particular, Dental caries and periodontal disease are the major causes for tooth loss[10-12].

1.2 Bone regeneration procedures

Successful repair of bone deficiencies is a major concerning topic in the oro-maxillo-facial (OMF) field. To restore the bone tissue volume is challenging because oro-facial functions, such chewing and swallowing, are delicate, due to the complex anatomical structures of the jawbones and the oral mucosa[3,13-15].

Guided bone regeneration (GBR) procedures have become everyday treatment in order to allow the placement of dental implants or the periodontal regeneration; GBR is based on the application of membranes and grafting materials[16,17].

To achieve a successful GBR, there are various indications, different alternative techniques, and numerous 'biologically active' agents and biomaterials currently used in dental practice[16-19].

Mostly of GBR techniques require special barrier membranes to protect defects from the ingrowth of soft tissue cells so that bone progenitor cells may develop bone uninhibited. Membranes can be resorbable or non-resorbable; resorbable are usually made by polylactic acid (PLA) or L-polylactic acid (PLLA), porcine collagen or polyglactin. Non-resorbable membranes are usually made by titanium-reinforced expanded polytetrafluoroethylene (e-PTFE)[20].

Among the graft materials there are more options, autogenous bone grafts are considered to be the material of choice for GBR, indeed it is defined as the "gold standard", as it has the biocompatibility, osteoinductive and osteoconductive properties, without immunological reactions and extra costs for purchasing biomaterials[21-23]. However, their use leads to an additional surgical intervention, possible complication of the donor site and a limited amount of graft[21-23].

Other bone substitutes are: allografts, xenografts or alloplastic graft materials.

Both of these three substitutes possess advantages and disadvantages, and they can be used in combination with autografts or alone, according to the chosen GBR technique[17,19,22].

1.3 Tissue Engineering and Regenerative medicine

Tissue engineering (TE) and regenerative medicine (RM) are emerging fields focused on the development of alternative strategies for tissue or organ repair that made significant progress in the last years[24,25].

TE provide new regenerated tissues by the appliance of cells, scaffold and growth factors, alone or in combination; nowadays RM has made exceptional progress leading to the regeneration of numerous organs and organ systems by using the capability of stem cells to differentiate into specialized cell types[26-28].

Stem cells are promising tools for tissue repair, due to their extensive proliferation and differentiation plasticity, unique ability that make them able, in theory, to regenerate injured tissues[24,29].

Stem-cell-based bone tissue engineering has demonstrated potential; the ideal cell populations are autologous mesenchymal stem cells (MSCs) from adult sources[30].

Defined as a population of non-hematopoietic fibroblast-like cells, MSCs are a self-renewing populations which express the ability to differentiate into multiple lineages, including osteoblasts, adipocytes and chondrocytes[24,31,32].

The main difficulties of the use of MSCs remains the identification of accessible sites within the human body where can be collected an adequate amount of stem cells. Indeed, the number of MSCs is higher before the birth, but it decreases during the aging, reducing their presence in several "niches"[24,31,32].

MSCs they have been usually isolated from bone marrow and are defined as bone-marrow-derived mesenchymal stem cells (BM-MSCs), but the BM-MSCs possess some weakness, such as their difficulty of isolation, large trauma, high expense, and patient's low degree reception[33,34].

Recently, many niches of MSCs have been described in the oral cavity: the dental pulp from permanent (DPSCs) or deciduous teeth (SHED), the periodontal ligament (PDL), the apical papilla, the dental follicle and the gingival tissue (GMSCs)[35-39].

1.4 Dental pulp stem cells

DPSCs have been described for the first time by Gronthos et al in the 2000, which described the presence of neural crest-derived stem cells from the dental pulp of adult human body[35].

Neural crest-derived stem cells originate from the process that give rise to the dental laminae during the sixth week of the embryogenesis, when the ectoderm begins to proliferate. The ectoderm-mesoderm interactions lead to the development of tooth germs, where neural crest cells differentiate into the dental organ, dental papilla and dental follicle.

Consequently, dental pulp develops from both ectodermic and mesenchymal components, containing neural crest cells. These adult stem cells have been called DPSCs, when isolated from permanent teeth; while, when isolated from deciduous teeth, they are defined SHEDs (Stem Cells from Human Exfoliated Deciduous)[26].

As well as MSCs, DPSCs and SHEDs are clonogenic cells capable of both self-renewal and the capability to give rise to different specialized cell types[40].

Moreover, compared to the BM-MSCs, DPSCs and GMSCs are easier to be harvested and have demonstrated the ability to proliferate faster, to be mostly homogenous and to have excellent capacity to differentiate in osteogenic cells[33-35,40].

Indeed, since their first isolation, DPSCs and SHEDs have been widely investigated for their potential application in TE in the last decades; in vitro and in vivo results have shown the capability of these stem cells not only in bone tissue, but also in adipose tissue, dentin-like tissue, cartilage, hair bulb, nerves fibres[40]. In particular, DPSCs and SHEDs have been successfully applied for bone regeneration not only in animal models but also in human being[41-43].

In addiction, the presence of DPSCs have been investigated from tissues harvested from fractured teeth, teeth with caries or irreversible pulpitis, or aggressive periodontitis[44-47].

1.5 Gingival mesenchymal stem cells

Gingival tissue is composed of an epithelial layer and underlying lamina propria; as well as dental pulp and all the other craniofacial tissues of mesenchymal origin, these tissue develops from the cranial neural crest[48].

Gingival mesenchymal stem cells (GMSCs) have been isolated more recently than DPSCs, indeed, GMSCs were firstly described by Zhang et al. in 2009[49].

The GMSCs are a subpopulation of the gingival fibroblast and exhibited all the MSCs characteristics: self-renewal capability, multipotent differentiation, and immunomodulatory abilities both in vitro and in vivo[49,50].

It has been demonstrated that GMSCs are more superior to BM-MSCs: GMSCs are uniformly homogenous, proliferate faster than BM-MSCs without any growth factor, display stable phenotype, maintain normal karyotype and telomerase activity, and are not tumorigenic[51-53].

Clinically, it is extremely simple to collect gingival tissue by biopsy, contrary to pulpar or periodontal cells that require tooth extraction for harvest[50,52]. Furthermore, the regeneration of gingival anatomy usually takes place in a short time period after wounding, usually lead to a perfect healing of the gum without complication for the patients, representing another advantage[50,52].

Similar to other MSCs, GMSCs cultures can be induced to differentiate into osteo-, adipo- and chondrogenic lineages as well as to myofibroblasts in vitro[54]. Noteworthy, experimental studies have proved that GMSCs possess also the capability to develop mineralized tissues in vivo[55-57].

In addiction, as well as for the DPSCs, the presence of GMSCs has been proved also in inflamed and hyperplastic tissues[53,58].

1.6 Scaffolds

Not only the source of the cells is important but also the design and the formation of a structure able to support the migration and growth of cells is essential to achieve new tissue formation[25,59].

To achieve bone tissue regeneration is needed the use of a suitable scaffolds; the major function of scaffolds is to furnish temporary structural support for osteoprogenitor cells, and osteoinductive factors desired to repair bone defect[25,59].

Scaffolds are principally biodegradable, synthetic, three dimensional (3D) structures, emulating the extracellular matrix and containing macro- and micro-pores that guide cell adhesion, proliferation and differentiation[60,61].

To secure a high density of colonizing cells and to promote neovascularization when implanted in vivo, the scaffolds should possess excellent mechanical properties, extensive surface area and pore size distribution along with highly interconnected porous structure[62,63].

Thermally induced phase separation (TIPS) can be used to produce a well interconnected porous scaffold; indeed, this technique allows to obtain different porous materials as scaffold architectures simply changing one or more experimental processing parameters and system properties[61,64].

"TIPS technique is based on thermodynamic demixing of a homogeneous polymer-solvent solution into a polymer-rich phase and a polymer-lean phase, usually by either exposure of the solution to another immiscible solvent or cooling the solution below a binodal solubility curve"[64].

Various polymers have been employed to create scaffolds by mean of TIPS technique; Poly(L-lactide) (PLLA) has been extensively used as a scaffold material for bone tissue engineering due to its superior mechanical properties, well-known biodegradability and biocompatibility[65-67].

1.7 Aim

The aim of the study is to provide the evidence of a new potential sources of MSCs for bone regeneration in dentistry. The DPSCs and the GMSCs were isolated from periodontally compromised teeth and their corresponding inflamed gingiva (P-DPSCs and P-GMSCs).

The inflammatory effects on human dental stem cells has been evaluated; we compared the MSCs markers, MSCs gene profile, proliferation and in vitro differentiation ability of the P-DPSCs and P-GMSCs compared to healthy teeth (H-DPSCs and H-GMSCs). We investigated if pro-inflammatory microenvironment negative affects dental MSCs characteristics and their capability and we speculated about a closer link between chronic inflammation and bone formation.

Furthermore, we evaluated the capability of P-DPSCs and P-GMSCs to develop vital bone tissue in vivo, in comparison to H-DPSCs and H-GMSCs.

In addiction, P-DPSCs and P-GMSCs, as well as H-DPSCs and H-GMSCs, have been seeded on 3D PLLA scaffolds obtained with the TIPS technique to study their ability to form new mineralized bone tissue in vitro.

CHAPTER 2

Materials and Methods

2.1 Ethics

All the procedures reported were approved by the Internal Ethical Committee of the University Hospital A.U.O.P "P. Giaccone" of Palermo (Internal registry: 5/2014). Patients signed an informed consent form before recruitment for the study.

2.2 Dental pulp and gingival tissue extraction

Dental pulp was extracted from teeth of healthy adults aged 18-75 years.

The eligibility criteria for participants were the following: extraction needed for molars suffering from severe periodontal disease (mobility grade III) (Test group), extraction needed for wisdom teeth for orthodontic reasons (Control group), no suspected or visible pregnancy in females, positive response to the vitality test performed on teeth to be extracted.

Before extraction, each patient had to rinse his or her mouth with 0.2% chlorhexidine for one minute (Meridol®, Gaba Vebas S.r.l., Rome, Italy) to decontaminate the oral cavity. Gingival tissue was collected while the patient underwent oral surgery procedures for tooth extraction.

2.3 Establishment of pulp dental and gingival cell cultures

All the samples were processed by Professor Giordano's research group (Laboratory of Regenerative Medicine (DIBIMIS)).

After surgery the pulpal or the gingival tissue was transferred to an RPMI culture medium (Sigma - Aldrich, Milano, Italy) enriched with 0.2 mg/ml gentamicin, 0.25 mg/ml levofluoxacin, 0.10 mg/ml vancomicin, 0.25 mg/ml fluconazole in a 50 ml tube and within 24 hrs the samples were digested.

Digestion was carried out in a solution of 5 mg/ml collagenase G (Abiel, Palermo, Italy) and 2 mg/ml collagenase H (Abiel, Palermo, Italy), 4:1 respectively, 4 hrs at 37°C, in agitation. The digests containing primary cells from the pulp or the gingiva were centrifuged and transferred to a T25 cell culture flask (EuroClone, Milano, Italy) or a p60 dish culture (to which we referred as passage 0, p0). The cells were maintained in culture in RPMI culture medium enriched with 0.5µg/ml gentamicin, 0.25µg/ml levofluoxacin, 0.10µg/ml vancomicin, 0.25µg/ml fluconazole and 5% fetal bovine serum

and incubated at 37°C, in 5% of CO2. Primary cells were attached to the flask within 4-5 days. Once they reached 80% of confluence (in about two weeks) they were trypsinized and the subculture was started (passage 1, p1). By subculture p4 the antibiotic and anti-fungal cover was abolished (Expansion Medium: EM). The p1–p8 cells were used for the in vitro assays.

2.4 Colony-forming assay

To assess the colony-forming efficiency of the dental pulpal mesenchymal stem cells (DPSCs) and gingival mesenchymal stem cells (GMSCs), single-cell suspensions (p0) from the periodontally-compromised teeth and healthy donors were seeded in a six-well culture in RPMI with 10% FBS at a density of 300 cells/well and cultured at 37°C and in 5% of CO2. After 14 days, the cells were fixed in 4% paraformaldehyde, stained with 0.1% crystal violet. Only the cellular groups containing more than 50 cells were considered as colonies.

2.5 Cell proliferation curve and Population Doubling (PD)

Proliferation was assayed by Trypan blue (Sigma-Aldrich), according to the manufacturer´s instructions. The p2 GMSCs or p2 DPSCs from Healthy (H) or Periodontally-compromised (P) donors were seeded at a density of 4x103 cells/cm2. The p4 H-DPSCs or p4 H-DGMSCs with or without 20ng/ml IL-1β and 40ng/ml TNF-α were seeded in a 96-well culture at a density of 4x103 cells/cm2 cells and cultured up to 120 hours. The cell counts were performed by optical microscope observation after trypan blue staining every 24 hours during the incubation period. The doubling time (DT) was calculated according to the literature data (Roth V. 2006 on the website http://www.doubling-time.com/compute.php.). Three sets of experiments for each sample were used for calculations.

2.6 Cytokine toxicity assay

The p4 H-GDPSCs or p4 H-DGMSCs with or without 20ng/ml IL-1β and 40ng/ml TFN-α were seeded in a 96-well culture at a density of 4x103 cells/cm2 cell and cultured for up to 72 hours. Cell viability was evaluated by UV absorption spectrum at 550 nm at 24, 48 and 72 hours using a micro-plate reader, after 3-(4,5-Dimethylthiazol-2-yl)-2,5-diphenyltetrazolium bromide (MTT) incubation for 4 hours at 37°C. Bone Marrow-derived Mesenchymal Stem Cells (BM-MSCs) were used as positive control.

2.7 Cell cycle cytofluorimetric analysis

Single cell suspensions of H-DPSCs, P-DPSCs or H-GMSCs and P-GMSCs were obtained and DNA content analysis was performed, according to Nicoletti's protocol. Briefly, 1x106 cells were fixed in 70% ethanol, rehydrated in PBS and then resuspended in a DNA extraction buffer (with 0.2 M NaHPO4, 0.1% Triton X-100 and, pH 7.8). After staining with 1μg/ml of propidium iodide (PI) for 5 minutes, fluorescence intensity was determined with a FACS Calibur flow cytometer (Becton-Dickinson, New Jersey, USA). Data acquisition was performed with CellQuest (Becton Dickinson)

software, and the percentages of G1, S, and G2 phase cells were calculated with the MODFIT-LT software program (Verity Software House, Inc.). The Proliferation index (PI) was expressed as % G2 + % M.

2.8 Surface marker cytofluorimetric analysis

The H-DPSCs, P-DPSCs or H-GMSCs and P-GMSCs were harvested and filtered through a 40µm filter mesh and suspended at the concentration of 1x106 cells/ml. Then 100 µl of cell suspension containing 5x105 cells were used for each cytofluorimetric test.

2.9 Flow cytometric Immunophenotyping

Human anti-HLA-DR, human anti-CD34, human anti-CD45 monoclonal antibodies were tested on H-DPSCs, P-DPSCs or H-GMSCs and P-GMSCs and were detected with the appropriate secondary antibody (Table 1). The incubation conditions were in accordance with the manufacturer's instructions. Unstained cells were used as a negative control. BM-MSCs were used as a positive control.

2.10 Stem cell phenotype

The cells were tested for expression of Stro-1, CD146 and CD29 and SSEA4 surface MSC markers, with the appropriate human anti-monoclonal antibody. The antibody dilution, incubation and detection conditions are shown in Table 1.

All reaction mixtures were then acquired with a FACS Calibur flow cytometer (Becton-Dickinson, New Jersey, USA) and analyzed with the CellQuest Pro software. Unstained cells were used as negative control.

Isolation of total RNA, Reverse-PCR, Real Time PCR and semi-quantitative PCR Total RNA was extracted and purified using the E.Z.N.A. Total RNA Kit I (Omega Bio-Tek Inc Georgia, USA) according to the manufacturer's instructions. RNA quantity and quality were assessed using Nano Drop 2000 (Thermo Scientific); 2µg of MSC total RNA were reverse-transcribed to cDNA in a volume of 20µl with Oligo dT primers (Applied Biosystems, California, USA) and the Reverse Transcriptase Rnase kit (Improm II, Promega, Wisconsin, USA).

2.11 Real-time quantitative PCR (qRT-PCR)

qRT-PCR primers were purchased from Qiagen (QuantiTect® Primer Assays, Qiagen, Milan, Italy) and Eurofin MWG (Biotech, Germany) and are listed in Table 2. All reactions were performed using the Quantitect SYBR Green PCR Kit (Qiagen, California, USA) using the RotorGene Q Instrument (Qiagen, California, USA). Each cDNA sample was mixed with specific primer sets and PCR master mix. The PCR reactions were performed using the following parameters for 40 cycles: denaturation at 95°C for 3 minutes, 95°C for 20 seconds, annealing at 60°C for 30 seconds and elongation at 72°C for 60 seconds. Reactions were performed at least in triplicate. The specificity of the amplified products

was determined by the melting peak analysis. The relative quantification model with efficiency correction was applied to normalize the expression of the target gene to β-actin (used as a housekeeping gene) and to compare gene expression with BM-MSCs (used as a positive cell control), on Rest2009 software (Relative Expression Software Tool, Qiagen)[33]. The results were described as histograms using the GraphPad Software, Inc., California.

qRT-PCR analysis for the stem genes was also performed after pro-inflammatory cytokine treatment: H-DPMSCs or H-GMSCs were incubated with 20ng/ml IL-1β and 40ng/ml TNF-α up to 72 hours. The forward (F) and reverse (R) primer sequences used for the reactions of amplification are listed in supplemental materials (Table 2).

2.12 Semi-quantitative PCR

To determinate the expression of runx-2 (Runt-related transcription factor 2) and actin-depolymerizing factors (ADFs):1µl complementary DNA was added to a 50µl reaction containing 5µl 10x reaction buffer, 50mmol/L MgCl2, 1µl dNTPs, 50pmol sense and anti-sense primers and 0.5 U Taq Gold DNA polymerase. The reactions were carried out according to the following protocol: I) 95°C for 10 minutes, II) 35 cycles at 95°C for 45 seconds, III) primer-specific annealing temperature for 45 seconds, IV) 72°C for 45 seconds, V) a final extension cycle at 72°C for 7 minutes, followed by a termination cycle at 4°C.

The primers were purchased by MWG and the sequences were the following: runx-2 F: 5'-TACGACTGGACGCTGGTGC-3', R: 5'-TTCATGGGTCGCTTGACGT-3'; Profilin-1 (Pfn-1) F: 5'-ACCCGGAAACAAGAAGAC-3', R: 5'-ACTGGTCCGATAACCTCCCA; Cofilin-1 (Cfl-1) F: 5'-TGCGGCTCCTACTAAACGG-3', R: 5'-ACGCACCTTCATGTCGTTGA-3'; Vinculin (Vcl) F: 5'-ATGTCTCCTATATCCTGGTTTTTGT-3', R: 5'-GCAGGAAGTGTCCTTCAGAC-3'

The protein-interaction networks (PIN)

Network analysis was performed on the heat shock proteins (HSPs) and ADFs using the STRING (Search Tool for the Retrieval of Interacting Genes/Proteins) found at the website <http://string-db.org/>.

2.13 Bone in vitro formation

5x103/cm2 H-DPSCs or H-GMSCs were incubated in EM with 20ng/ml IL-1β and 40ng/ml TNF-α (cytokine precondition treatment). After 72 hours the medium was replaced with homemade osteogenic differentiation medium (ODM). 5x103/cm2 H-DPSCs, P-DPSCs or H-GMSCs and P-GMSCs were cultured in ODM. After 21 days of culture in the ODM, the cells were stained with Alizarin Red S (Sigma-Aldrich, St. Louis, USA) to detect calcium deposits. Briefly, the medium was removed and the cells were fixed with 4% formaldehyde solution for 30 minutes, and after fixation rinsed twice with distilled water and stained with 2% Alizarin Red S (pH 4.2) for 3 minutes. After observation under a light optical microscope, the images were acquired by Nikon DS-fi1 cam and for quantification of the

calcium deposits ImageJ software was used (https://imagej.nih.gov/ij/docs/concepts.html). The ODM consisted of DMEM supplemented with 15% FBS, 10-4 mM dexamethasone (Sigma-Aldrich, St. Louis, USA), 10 mM glycerophosphate (Sigma-Aldrich, St. Louis, USA) and 0.05 mM ascorbic acid (Sigma-Aldrich, St. Louis, USA)[24].

2.14 PLLA Scaffold preparation

The Poly-L-lactic Acid (PLLA) scaffolds were produced by Professor Brucato's research group (Department of Civil, Enviromental, Aerospace, Materials Engineering (DICAM) of the University of Palermo).

Thermally Induced Phase Separation technique (TIPS) was employed in order to produce well interconnected porous structure, following procedures already reported in literature[64,68].

A homogeneous ternary solution composed of PLLA, dioxane and deionised water was prepared with a constant dioxane to water ratio of 87/13 (wt/wt); the polymer concentration was chosen to be 4% (wt/wt). The cloud point of the solution was at 40°C, so the solution was initially kept at 60°C.

In order to establish the ideal porous structure for the DPSCs e GMSCS cells, different scaffold were prepared with different thermodynamic pathways and related different microporous structures.

All the scaffolds were prepared using a cylinder aluminium sample holder (diameter 6 mm, height 30 mm).

The first two types of scaffolds were prepared using a binodal de-mixing technique; first the solution was hot poured into the sample holder, then the sample holder was immersed into a thermostatic water bath, in order to suddenly decrease the temperature to 30°C (scaffold a) or 25 °C (scaffold b) for 15 min (de-mixing time),

Subsequently, in order to freeze the as-obtained structures, a quench by pool immersion in an ethyl alcohol bath at a temperature of -20°C for 15 min was performed. Then, the scaffolds were extracted from sample holder, washed into deionised water for 24h and dried at 20°C under vacuum overnight, in order to completely eliminate any solvent trace.

The microporous structure of the obtained scaffolds were approximately 150 μm (scaffold a) and 50-70 μm (scaffold b).

After the initial in vitro studies, a different protocol was adopted consisting of a spinodal decomposition technique (scaffold c). This procedure was slightly different from the first described before. After that the sample holder was filled with the ternary solution, it was immersed into a thermostatic water bath at 0°C for 10min; afterwards a teflon coating was applied and the as-obtained structure was cooled in an ethanol bath at -20°C for 15 min. The as-obtained structure were then washed and dried as described before. With this second technique achieved scaffolds with 5-20 μm micropores were achieved.

2.15 Scaffold characterization before seeding

Due to the cylindrical shape of the sample holder, the cylindrical 3D scaffolds were cut to obtain disks of a diameter of 6 mm and thickness of 2 mm.

The disks were sterilized in 70% ethanol (v/V) solution under vacuum for 18 h; subsequently four washes were carried out using with sterile PBS, to remove all the ethanol.

A solution of collagen (type I solution from rat tail,) in acetic acid (0.02N) at the concentration of 200μm/ml was prepared to coat the scaffolds, the solution was filtered with 0,2 μm filters.

To achieve the collagen coating, the scaffolds were immersed in the obtained solution for 90 min at 37°C. Afterwards the scaffolds were washed with PBS and kept in culture medium until the cell seeding.

2.16 GMSCs seeding

To text the capability of the MSCs chosen in this project, initially it was decided to employ only the P-GMSCs.

The in vitro test was conducted by seeding a cell suspension, at density of 1x105 GMSCs, on the top of scaffolds a and b (respectively with 150 and 50/70 μm micropores).

After the seeding the scaffolds were incubated at 37°C for 90 min without the culture medium to promote the cell adhesion; then the scaffolds were placed into 24-well plates and 1ml of complete DMEM was added. Incubation was left at 37°C and 5% of CO2.

The same procedures were applied to test the scaffolds c; regarding this second in vitro examination, two different volume of the solution containing the P-GMSCs were used: 20 μl and 15 μl.

Viability of the P-GMSCs was investigated at established points (after 12h, 40h and 120h).

2.17 Cell Counting Kit-8 assay

The Cell Counting Kit-8 (CCK-8) assay was utilized to detect the viability of P-GMSCs seeded on scaffolds a and b. The scaffolds were placed in 96-well plates, and the absorbance at 450 nm was detected at 1–6 days after seeding.

2.18 Alamar Blue cell viability assay

The scaffolds c were transferred into new 24-well plates with 500 μl of Alamar Blue solution and DMEM, then plates were incubated for 3h at 37°C.

Then the solution incubated with the scaffolds was transferred in a 96-well plates (100 μl) and the fluorescence was evaluated by a spectrophotometer.

2.19 Cell vitality assay

To text the cell vitality assay of scaffolds c were used Acridine orange (AO) and ethidium bromide (EB). The dye mix for the EB/AO staining was 100 μg/ml acridine orange and 100 μg/ml ethidium bromide in PBS.

The scaffolds tested were firstly placed in new 24-well plates and washed four times with PBS (100 µl), every wash cycle was of 5 minutes by mean of an oscillating surface.
EB/AO dye mix (30 µl) was added to each well for 5 min, and cells were viewed under the fluorescence microscope using FITC and TRITC filters.

2.20 DAPI assay

The investigated scaffolds were placed in 24-well plates and washed three times with PBS (100 µl); then the scaffolds were fixed in 3,6% formaldehyde in PBS for 15 minutes. After washing in PBS, samples were stained with 1:100 µl DAPI in PBS for 1 minute, finally the scaffolds were observed under the fluorescence microscope.

2.21 In vivo implantations

All experimental procedures and protocols were approved by the "OPBA – Organismo Preposto al Benessere degli Animali" of the "A.Mirri" Experimental Zooprophylactic Institute of Sicily (approval No. 1061/2015) and by the Italian Minister of Health (approval No.1185/2015).
All the surgical procedures were performed at the "A.Mirri" Experimental Zooprophylactic Institute of Sicily.
6-week-old immunodeficient nude mouse (NU/NU) were used for the study, in each mouse were injected subcutaneously on the dorsal surface (n=2 per mouse) the cells suspension (fig.1).
In detail, in the first trial, approximately 10^5 cells of DPSCs or GMSCs from healthy and periodontal donors were suspendend in 100µl of differentiation medium, for each group were prepared one suspension with osteogenic differentiated cells and one suspension with undifferentiated cells, as control. Indeed, four mice were used to text the capability of the cells to differentiate in vivo.
Mice were sacrificed and dissected at 4 weeks after cell transplantation.
In the second trial, the number of cells suspended were raised to $2x10^5$ cells as well as the volume of the solution, that was raised to 200 µl. For each group were prepared the same suspensions, and four mice were used also for this text.
Mice were sacrificed and dissected at 8 weeks after cell transplantation.

2.22 Statistical analysis

All assays were performed in triplicate. The data were reported as means ± SD and compared using the appropriate version of Student's unpaired t-test or One way Anova analysis of variance and post Tukey's multiple comparison test. $p < 0.05$ was considered statistically significant.

CHAPTER 3

Results

3.1 Inflamed dental tissue-derived MSCs

The DPSCs and GMSCs were isolated from 49 patients. The subjects were divided into two major groups: 1) periodontally-compromised group (P, n=37, test group) and 2) healthy group (H, n=12, control group). For each patient pulpal and gingival tissues were extracted. Nine of the total samples (n=5 test group; n=4 control group) were unsuccessfully processed, because of a high grade of bacterial contamination. For all 40 samples, after enzymatic digestion a cell suspension was generated. The first plastic adherent cells were detected from all cultures within seven or ten days of preparation. Initially primary cells from healthy tissue grew faster than those from test group. The cell cultures (p0) appeared heterogeneous in shape and size, and the cells showed the ability to grew out from tissue no totally digested and to form a clone-like growth (Fig.2 a-b, e-f). Generally, in culture progress, gingival cells reached confluence at day 15 (12-18 days) and pulpal cells at day 20 (14-26). All the primary cells showed typical fibroblast-like morphology and they were homogeneous in shape and size (Fig.2 c-d, g-h).

After they reached confluence, the cells were harvested and sub-cultured. From culture p1, a modest change in growth behaviour was observed: although the MTT assay revealed no difference ($p< 0.05$) in the growth rate, the P-DPSCs and P-GMSCs proliferated faster than healthy control cells. The doubling time (DT) was established at 34.37 ± 5 hrs vs. 28.83 ± 2 hrs for H-DPSCs vs. P-DPSCs, respectively; and at 29.13 ± 4 hrs vs. 26.22 ± 8 hrs, for H-GMSCs vs. P-GMSCs, respectively. The cell cycle analysis assigned a proliferation index (P.I.) G2M+S of 7.7% vs. 3.43%, respectively for P-DPSCs vs. H-DPSCs and a P.I. of 23.85% vs. 10.2%, respectively for P-GMSCs vs. H-GMSCs. The difference in P.I. H-DPSCs vs. P-DPSCs and H-GMSCs vs. P-GMSCs was statistically significant (Fig.3).

3.2 Test and control dental pulp and gingival cell express putative mesenchymal stem cells markers; they were negative for hematopoietic differentiation clusters and showed a stem gene profile

The isolated cells did not display any hematopoietic surface markers (CD34 and CD45) and HLA-DR. A slight increment was detected in the expression level of CD34 in test group, but was not statistically significant ($p>0.005$) (Fig.4). We analyzed the expression of putative mesenchymal surface stem cell markers

Stro-1, CD146, CD29 and SSEA4 by flow cytometry, compared to BM-MSCs (positive control, not showed) (Fig.5). In all samples, CD29 remained highly positive (about 100%). A higher Stro-1+/CD146+/SSEA-4+ cell population was detected in P-DPSCs and P-GMSCs than in the respective healthy controls ($p<0.05$) (Tab.3).

We compared the stem molecular expression pattern in the H-DPSCs and H-GMSCs, P-DPSCs and P-GMSCs. Expression analysis showed significant differences in ABCG2, CD105 and in OCT4 and SOX-2 mRNA levels in GMSCs vs. DPMSCs, and in P-GMSCs vs. H-GMSCs. Generally, the MSC markers were consistently more highly expressed in dental MSCs than in BM-MSCs (Fig.5c).

3.3 The pro-inflammatory cytokine cocktail could facilitate dental pulp and gingival mesenchymal stem cells expansion in vitro

We investigated the effect of pro-inflammatory cytokines IL-1β and TNF-α.

After 72 hours of treatment, no cytotoxic effect on cells was detected and by contrast we found increased proliferation. In this connection, MTT analysis showed an increment in the percentage of vital cells and a decrease in DT was detected in H-DPSCs and H-GMSCs treated with IL-1β and TNF-α, miming a P-DPSC and P-GMSC proliferation curve (Fig.6 a-b).

3.4 Inflammation and stem cell gene profile correlation

To investigate whether the inflammation environment affects stem gene profile, a real-time PCR analysis was performed to compare H-GMSCs and H-DPSCs after 20ng/ml IL-1β and 40ng/ml TNF-α up to 72 hours treatment versus no treated H-GMSCs and H-DPSCs. In figure 6c and 6d, the histograms represent the mRNA levels expressed as a fold change (FC). In cytokine-treated H-GMSCs and H-DPSCs all MSC markers showed an increase of about 1.5 FC respect to H-GMSCs and H-DPSCs.

We found a statistically significant increase of about 1.52 and 1.37 FC in ABCG2, 1.19 and 1.6 FC in CD105, 1.18 and 1.77 FC in NANOG, 1.77 and 1.14 FC in OCT4, 2.89 and 1.83 FC in SOX-2, respectively in H-DPSCs plus cytokines vs. H-DPSCs and H-GMSCs plus cytokines vs. H-DPSCs ($p<0.05$).

3.5 Bone in vitro formation: Inflammation – cytoskeleton modulation – osteogenesis

To evaluate the effect of the inflammatory condition on osteogenic differentiation potential in vitro, H-DPMSCs and H-GMSCs treated with IL-1β and TNF-α for 72 hours were cultivated in the ODM and compared to P-DPSCs and P-GMSCs not cytokine-treated. After 21 days of differentiation culture procedure, phenotype and gene analysis were performed. As shown in figure 7a and 7b the alizarin red-positive area indicated a higher amount of calcium deposits in treated H-DPSCs, H-GMSCs and in P-DPSCs, P-GMSC compared to their healthy controls.

3.6 Inflammation increases the expression of differentiation-associated genes

A computational STRING investigation brought to our attention an interaction between inflammation

and cytoskeleton remodeling (fig.7c). To investigate whether the increase in osteogenic potential was correlated with both alteration of inflammation-related gene expression and actin modulation, we examined several HSP and ADF genes. After ten days of osteoblastic differentiation culture the mRNA levels of runx2, vcl, cfn-1 and pfn-1, hsp90, hspA9 and txn-1 expression were observed.

Confirming the higher osteogenesis in inflamed conditions, mRNA level increments of runx2 (specific osteoblastic nuclear factor) in P-DPMSCs, P-GMSCs and cytokine-treated dental MSCs were found. At the same time, we detected a decrease in cofilin-1 and profilin-1 expression and an increase in vinculin-1, hsp90, hspA9 and txn-1 in P-DPMSCs, P-GMSCs and in treated dental MSCs (fig.7d-e).

3.7 Scaffolds preparation and CCK assay

A homogeneous ternary solution of L-polylactic acid (PLLA) was used to create porous scaffolds via TIPS technique. All the produced scaffolds were analysed by mean of the SEM. From the sample holder-like scaffold were made PLLA disks, with a diameter of 6 mm and a thickness of 2 mm. The surface analysis of the samples allowed to define the surface area available for each scaffold, which was approximately equal to 10 cm2. In addiction, before the cell seeding, all the scaffolds were sterilized, as described before, and coated with collagen type I (200μm/ml).

The first scaffolds prepared (a and b) presented bigger micropores than scaffolds c, in detail: a) 150 μm, b) 50/70 μm, c) 5/20 μm.

The decision to create scaffold with smaller micropores was taken after the CCK assay of the scaffolds a and b. Cell culture tests carried out on these supports showed a quick decrease of the number of viable P-GMSCs cells seeded on the surface of the scaffolds during the examined culture period (10 days) (fig. 8).

For these reason, new scaffolds with smaller pores, (5/20 μm), were produced.

The new scaffolds presented smaller micropores and high degree of interconnection (fig 9 and fig 10).

Moreover, due to the results of the CCK assay, it was decided to seed 75000 cells for scaffold; so a cell suspension with 1x105 P-GMSCs for microliter density was seeded on every scaffolds. All experiments were performed in triplicate

3.8 2D Alamar Blue assay

The observation of the P-GMSCs growth showed a slow growth, strictly dependent to the cell density in the plates.

For that reason, in order to evaluate the ideal cell concentration to achieve a rapid cell growth on the scaffolds, a 2D Alamar Blue assay was carried out on P-GMSCs cells seeded at different concentrations.

In the fig. 11, it is possible to observe the P-GMSCs cell growth at different times. It was possible to observe how this cell type tends to stretch to make contact with neighbouring cells, at low cellular

density. Moreover, some P-GMSCs assumed a more similar astrocytes-like phenotype, as shown in fig. 12.

The results in fig. 13 showed a faster cell growth when the cell concentration was greater the 7500 cell/cm2. These data were essential to establish the ideal cell concentration for the successive seeding; additionally, it was define that the ideal dimension of the flasks was of 25 cm2.

3.9 3D Alamar Blue assay

The Alamar Blue assay, as described before, was used to evaluate the cell growth (fig. 14). The data showed the continuous cell growth in the studied period (120h), in which there was a doubling of the cells number present in the scaffold c. Comparing this curve with the previous one, related to the scaffold a and b, it is evident the difference in terms of cell growth between the two groups of the scaffolds.

3.10 AO/EB vitality assay

The observation of the scaffolds c through fluorescence microscopy at 72h confirmed a high level of cell viability (fig. 15). Indeed the red spot, related to non-viable cells, are few and circumscribed to few areas of the examined scaffolds.

3.11 DAPI assay

By nuclear staining and fluorescence microscopy, it was possible to observe the P-GMSCs distribution on the scaffolds c.

The acquired images, taken in different regions of the seeded scaffolds, showed that the cells are distributed homogeneously over the entire scaffold's surface (fig. 16).

3.12 In vivo studies

In the first animal study group was not observed bone formation at 4 weeks after cells transplantation (fig.17).

So, in the second study group, it was decided to increase the number of cells suspended, the volume of the cells suspension and the period of time before the sacrifice of the animals. Again, in the second animal study group was not observed bone formation at 8 weeks after cells transplantation (fig.18).

In both the animals were not presented any bone formation neither inflamed tissue formation.

CHAPTER 4

Discussion

For decades now extraordinary interest has matured in the field of MSCs because of their differentiation potential, which has led them to be used in TE, RM and cell and gene therapy for clinical applications. The search is ongoing for the best MSC tissue source. The elective tissues for this purpose are bone marrow and adipose tissue, although isolation of these MSCs may be an invasive procedure for patients and donors. In view of this, the possibility of isolating MSCs from discarded tissue is a fascinating idea and MSCs from periodontally-compromised teeth could be a good alternative. Even though it has been shown in the literature that pro-inflammatory cytokines affect MSC properties, the effects of inflammation due to periodontitis and its progression on the characteristics of dental MSCs remain unclear[47,58,69].

In the present study, we confirmed the presence of MSCs in human dental pulp and gingival tissue harvested from periodontally-compromised teeth and for the first time, to the best of our knowledge, at the same time we compared simultaneously the stem features to DPSCs and the GMSCs harvested from healthy donors. The cells isolated from all groups showed a typical fibroblast-like shape and proved positive for the principle stem markers (Stro-1, CD46, CD29 and SSEA4) and they did not exhibit surface expression for any hematopoietic marker (CD34 and CD45). Our results suggest that the inflamed condition related to the periodontal status of the patients has no effect on dental MSC viability, whereas it seems to improve the growth ability and stem gene profile of DPSCs and GMSCs. This view is supported by pro-inflammatory cytokine precondition experiments that demonstrated that H-DPSCs and H-GMSCs are able to mimic P-DPSCs and P-GMSCs, displaying similar proliferation curves and gene expressions when treated with IL-1β and TNF-α.

P-DPSCs and P-GMSCs show a clear higher expression of the cardinal stem nuclear markers (NANOG, OCT4 and SOX-2) and ABCG2 (superficial marker) compared to both H-DPSCs and H-GMSCs and the internal positive control (BM-MSCs). Moreover, our data about H-DPSCs and H-GMSCs under pro-inflammatory conditions in vitro show that osteoblastic differentiation capacity is not only well preserved but also is significantly improved compared to not stimulated and is almost equal to the MSCs of the test group. This finding was confirmed by a more highly calcified extracellular matrix formation and a higher expression of runx2, a bone-specific transcription factor, in

the cytokine-treated H-DPSCs and H-GMSCs as well as in the P-DPSCS and P-GMSCs[70-72]. Furthermore, we found that in the inflamed environment the expression levels of profilin-1 and cofilin-1 decreased, whereas vinculin and hsp90, txn-1 and hspA9 permit stabilization of actin filaments.
It has already been shown that in inflammatory environments several mediators activate a set of biological processes such as cell survival, proliferation and cell differentiation in MSCs[73-76]. During lineage specific differentiation, human stromal stem cells exhibit significant changes in morphology and actin cytoskeleton organization[77-82]. ADFs bind to actin monomers and filaments, causing depolymerization of actin filaments and thus preventing their reassembly and decreasing osteoblastic differentiation[82-86]. Osteoblastic cytoskeleton reconstruction depends on the regulation of the actin polymerization status carried out by ADFs, including cofilin, profilin and vinculin[87-89].

In recent years, one of the most studied materials has been the PLLA, which, in the present study, was used to develop scaffold by mean of the TIPS technique. The scaffolds were prepared according to a previously published technique by Pavia et al[64,68], allowing the formation of foams with an ordered multilevel structure and average micropores size ranging from 150 μm to 5/20 μm.
After the first in vitro study on scaffold a (150 μm) and scaffold b (50-70 μm), we observed a quick decrease of the number of viable P-GMSCs cells seeded on the surface of the scaffolds during the examined 10 days of culture period. For these reason, a different protocol was adopted to devolp a new scaffolda smaller micropores (5/20 μm) and high degree of interconnection.
Once we have defined the size of the micropores of the scaffold by mean of the 2D Alamar Blue assay, we evaluate the ideal cell concentration to achieve a rapid cell growth on the scaffolds.
In the second in vivo study on scaffold c, P-GMSCs showed the capability to grow on PLLA scaffolds
It was observed that P-GMSCs tend to assume an astrocytes-like phenotype and showed a faster cell growth when the cell concentration was greater the 7500 cell/cm2. These data were essential to establish the ideal cell concentration for the successive seeding.
Due to the 3D Alamar Blue assay and the AO/EB vitality assay, the P-GMSCs have shown a good proliferation rate, a high level of cell viability and low cells mortality.
Furthermore, due to the DAPI assay, it was possible to observe on homogeneous distribution of the P-GMSCs on the scaffolds c.
Indeed, it could be assumed that PLLA scaffolds with 5/20 μm micropores promote the adhesion and the replication of P-GMSCs.

Regarding the in vivo study, in both the animals study groups were not presented any bone formation neither inflamed tissue formation, at 4 or 8 weeks.
Probably these results are related to the unstable carrier chose for the implantation of the cells; the skin absorption of the suspension was to fast, not giving to the cells the time needed to induce bone formation in vivo.

New in vivo studies are ongoing: cells suspensions of H-DPSCs, P-DPSCs, H-GMSCs or P-GMSCs were seeded on new scaffolds, with the same characteristics of scaffold c. After one week of in vitro osteogenic differentiation, the scaffolds were transplanted subcutaneously on the dorsal surface of 6-week-old immunodeficient nude mouse (NU/NU).

In conclusion, our results confirm that the chronic inflammatory microenvironment existing in periodontitis does not negatively affect the number of P-DPSCs and P-GMSCs and their stem cell marker profile. Pro-inflammatory cytokines permit a higher osteogenic differentiation potential, controlling the fate of MSCs through several regulatory mechanisms involving remodeling of cytoskeleton and stress response processes. Our data need further confirmation using enriched P-DPSCs and P-GMSCs engineered scaffolds with the same set of experiments as presented in this study (data in progress). The first results about the growth and differentiation potential of seeded cells "in and from" the inflammatory environment are very promising. In our experience, P-DPSCs and P-GMSCs appear to be a valid autologous MSC source. In addition, they are promising for in vivo applications in diseases with persistent inflammatory environment that generally harms the features and hinders the success of cell transplantation. From a clinical point of view, our findings confirm the feasibility of tissue engineering and regenerative medicine applications in vivo.

CHAPTER 5

Tables and Figures

5.1 Tables

PRIMARY ANTIBODY/ LOCALIZATION MARKER	CODE NUMBER	DILUTION	INCUBATION
Stro-1, surface	Thermo Fisher Sc, 39-8401	1:100	Overnight (o/n), room temperature (r.t.)
CD 146, surface	Milteny Biotec, 130-092-851	1:50	30 min, room
CD 29, surface	Milteny Biotec, 130-101-258	1:50	30 min, room
SSEA4, surface	Milteny Biotec, 130-98-371	1:100	30 min, room
CD-34, surface	Santa Cruz, sc-19621	1:50	o/n , r.t.
CD-45, surface	Santa Cruz, sc-28369	1:50	o/n , r.t.
HLA-DR, surface	Santa Cruz , sc-18875	1:50	o/n , r.t.
SECONDARY ANTIBODY	CODE NUMBER	DILUTION	INCUBATION
AlexaFluor 488	Life Technologies, Z25402	1:50	20 min, r.t.
AlexaFluor 594	Life Technologies, Z25007	1:50	20 min, r.t.

Table 1: Human anti-monoclonal antibodies list used in flow cytometry analysis for detection of MSC markers.

GENE	PRIMER SEQUENCE	CODE NUMBER
ABCG2		QT00073206
CD105		QT0001335
THY-1		QT00023569
CD73		QT00027279
NANOG		QT01844808
OCT4		QT00210840
SOX2	*F:5′- GGAGACGGAGCTGAAGCCGC-3′* *R:5′GACGCGGTCCGGGCTTGTTTT-3′*	MWG
HSPA9 (mortalin)	*F:5′-TACAGCAGATGGTGAGCGAC-3′* *R:5′-TGCTGTGTGCCCCAAGTAAT-3′*	MWG
TXN-1 (thioredoxin-1)	*F:5′- GTGAAGTCAAATGCACGCCA-3′* *R:5′-GCAGATGGCAACTGGTTATGT-3′*	MWG
HSP90AA1	*F:5′-GTGAAGTCAAATGCACGCCA-3′* *R:5′-GCAGATGGCAACTGGTTATGT-3′*	MWG

Table 2: The primer sequence list used for the amplification of MSC cDNA.

MSCs	MESENCHYMAL STEM CELL MARKERS			
	STRO-1	CD146	CD29	SSEA4
H-DPSCs	12.30 ± 2.32 %	18.95 ± 1.79 %	99.07 ± 0.5 %	18.31 ± 1.06 %
P-DPSCs	31.32 ± 3.32 %	37.80 ± 4.79 %	97.26 ± 2.38 %	27.33 ± 2.71 %
H-GMSCs	10.61 ± 1.37 %	73.34 ± 5.43 %	96.64 ± 5.08 %	17.72 ± 1.97 %
P-GMSCs	20.46 ± 2.18 %	86.54 ± 3.76 %	96.74 ± 3.68 %	31.56 ± 2.54 %
BM-MSCs	6.25 ± 2.2 %	44.89 ± 5.54 %	97.21 ± 0.89%	5.1 ± 1.53 %

Tab. 3 The MSCs marker level expressions in healthy and periodontally-affected DPSCs or GMSCs. Standard deviations (±).

5.2 Figures

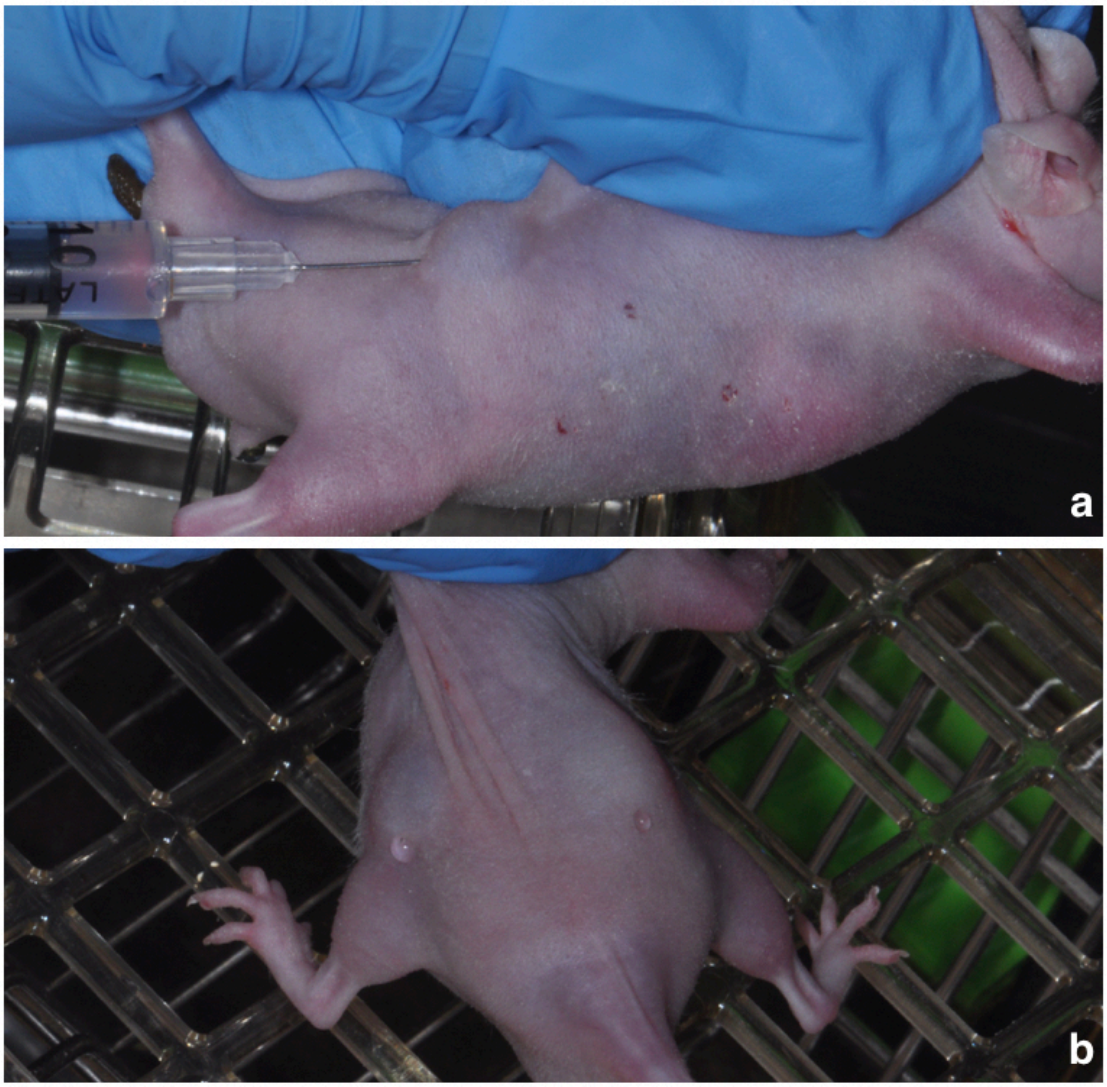

Fig. 1 Inoculation of the cells suspension subcutaneously on the dorsal surface of NU/NU mouse

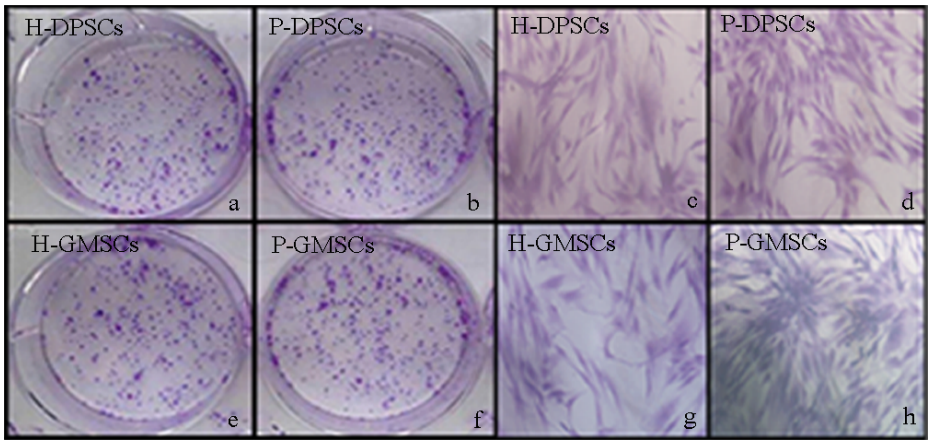

Fig. 2 Colony-forming unit assays and monolayer subculture: Representative image of pulpal or gingival mesenchymal stem cell colonies stained with crystal violet isolated from teeth of one healthy subject and one periodontal-affected patient. Figures a and b, e and f show the clone-like growth of H-DPSCs and P- DPSCs, respectively. Figures c and d, g and h show the typical fibroblast-like morphology of H-GMSCs and P-GMSCs (40x).

85x39mm (300 x 300 DPI)

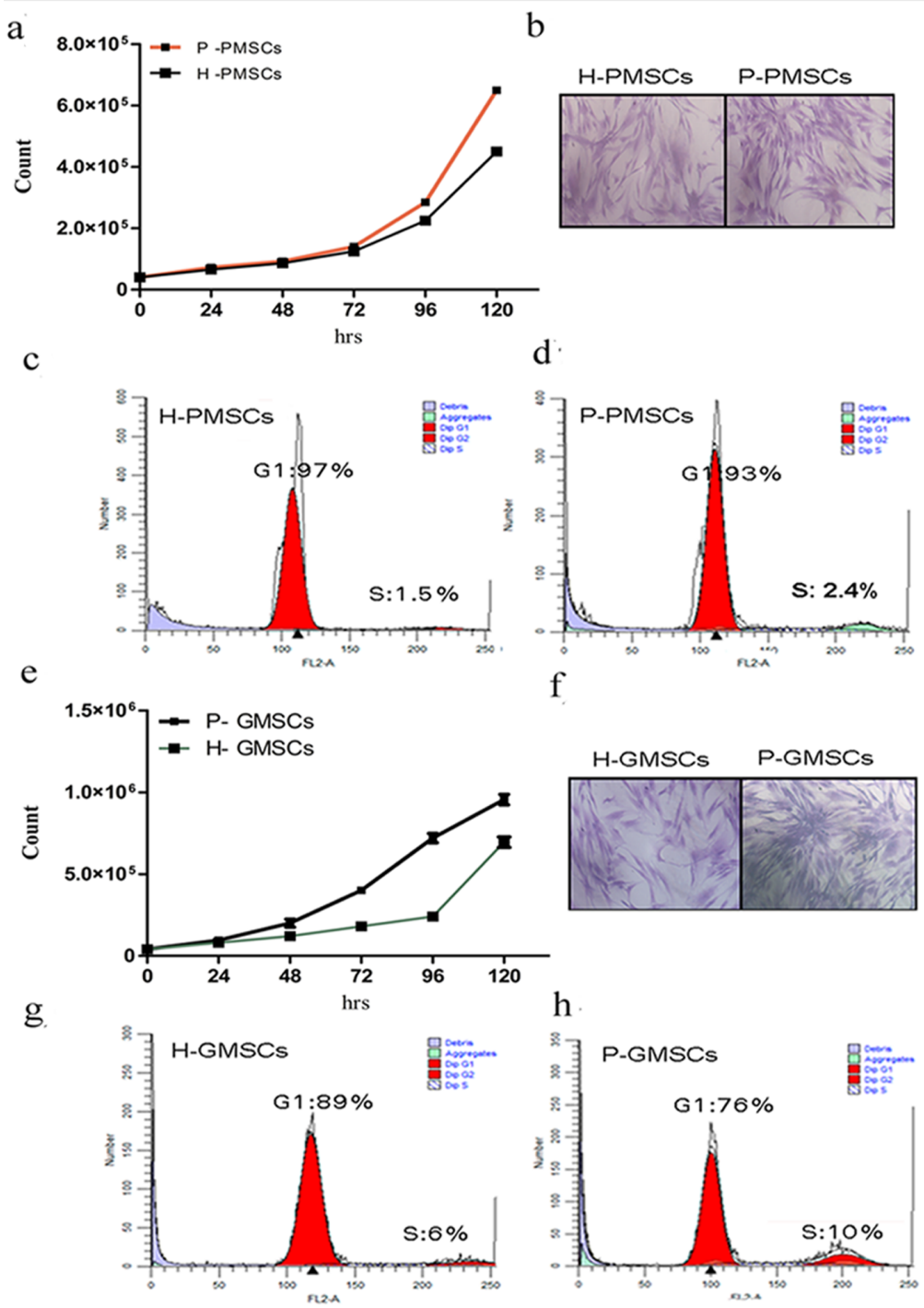

Fig.3 Proliferation curve and cell cycle analysis: In the upper panel: a) Cell growth curve of H-DPSCs and P- DPSCs evaluated with Trypan blue viability assay; b) From the typical fibroblast-like cell shape the higher P- DPSCs cellular density at 72 hrs is evident (40x); (c-d) A representative comparative analysis between cell cycle distribution of H-DPSCs and P-DPSC. In low panel: e) Cell growth curve of H-GMSCs and P-GMSCs with Trypan blue viability assay; f) H-GMSCs and P-GMSCs at 72 hrs; the P-GMSC cell density is higher than that of H-GMSCs (40x); (g-h) A representative comparative analysis of proliferative activity cell cycle distribution of H-GMSCs and P-GMSCs.

147x213mm (230 x 230 DPI)

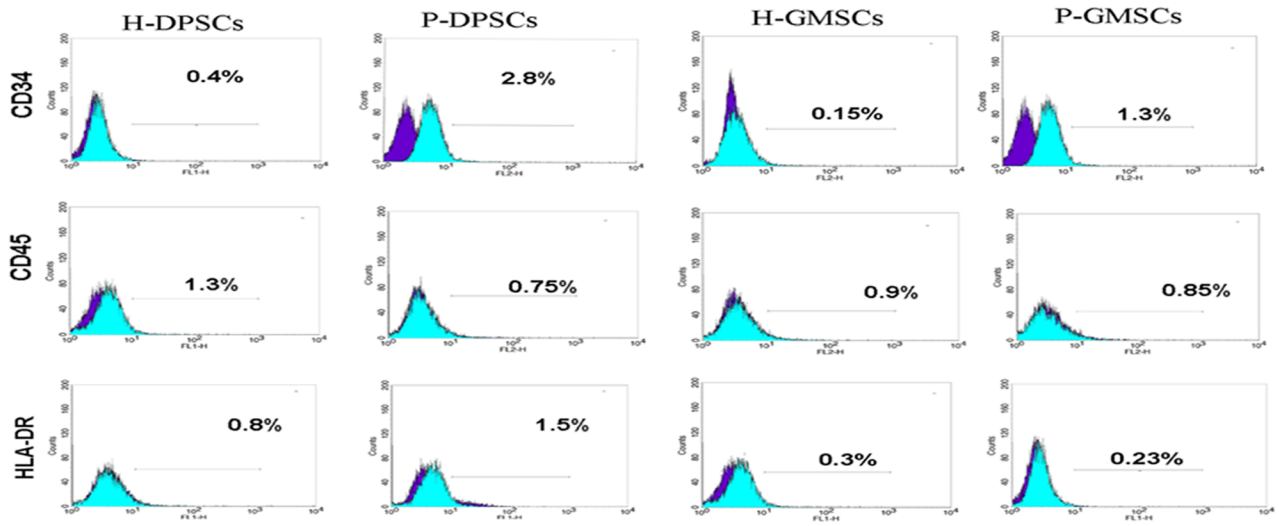

Fig.4 Immuniphenotype flow cytometric assay: Cells are negative for CD34, CD45 and HLA-DR. All fields are representative of one sample. The CD34 increment in a periodontal-affected sample was not statistically significant.

115x64mm (270 x 270 DPI)

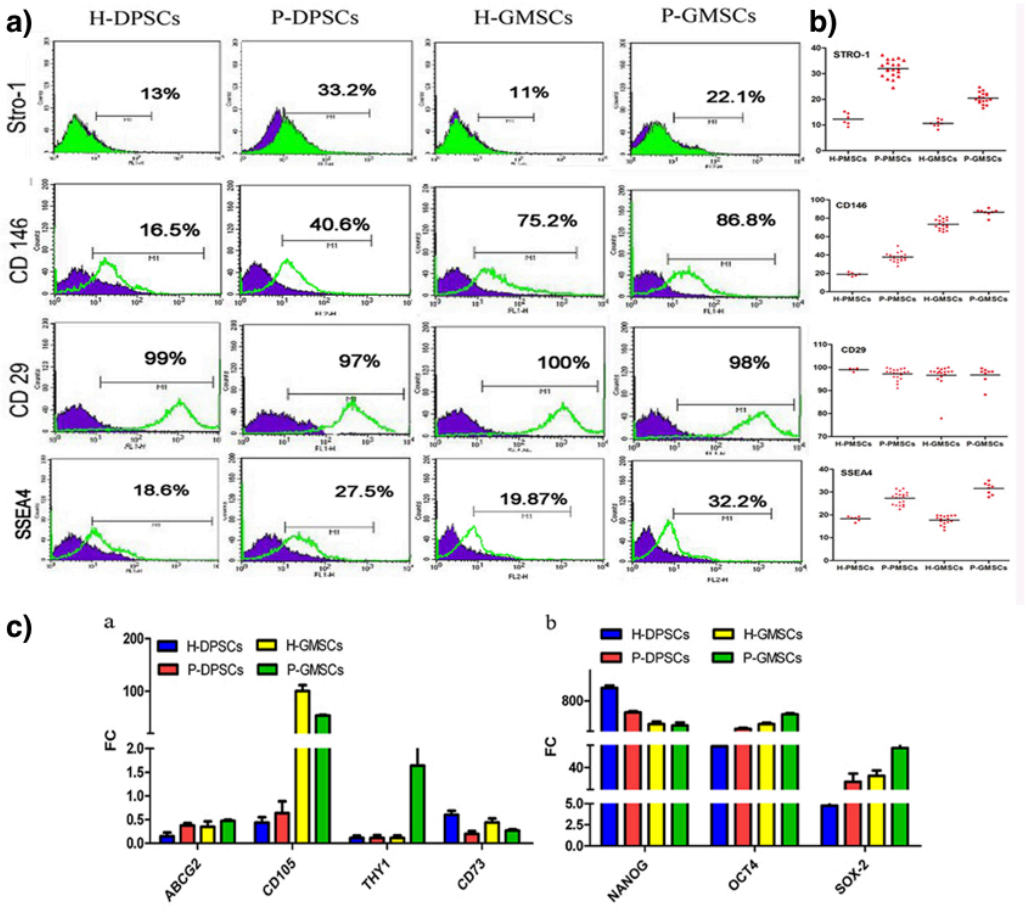

Fig.5 Stem cell feature analysis: a) A representative flow-cytometric analysis of periodontal-affected pulpal or gingival MSCs (P-DPSCs and P-GMSCs) in comparison to healthy controls (H-DPSCs and

H-GMSCs); b) The scatter dot plot graph represents the expression levels of mesenchymal stem cell markers (STRO-1; CD146; CD29 and SSEA4); c) the histograms represent a comparative qRT-PCR analysis of nuclear (on the left) and surface (on the right) markers in H-DPSCs, P-DPSCs, H-GMSCs and P-GMSCs. Actin-β was used as the housekeeping gene. FC (fold change). The mRNA expression of all analyzed genes was normalized against BM-MSCs (positive control).

147x210mm (270 x 270 DPI)

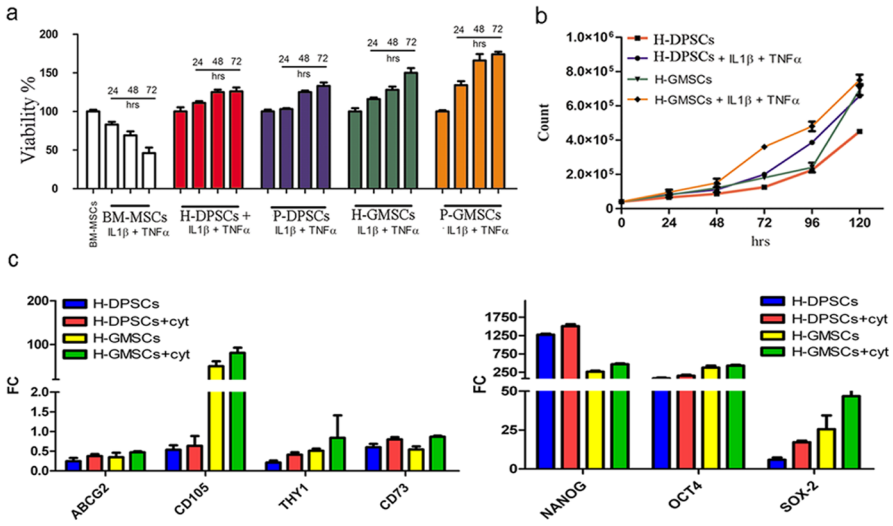

Fig.6 Two cytokines promote H-GMSC and H-DPSC expansion. a) Cytotoxicity assay: H-DPSCs, H-GMSCs without and after cytokine treatment; b) Cell growth curve of H-DPSCs and P-DPSCs without and after cytokine treatment evaluated with Trypan blue viability assay; c) Comparative analysis of nuclear (on left) and surface marker expression (on right) in H-DPSCs and H-GMSCs with or without cytokine treatment (20ng/ml IL-1β and 40ng/ml TNF-α for 72 hrs).
BM-MSCs: positive control; β-actin: normalized gene.
Mean values ± SD of all samples studied are reported. Error bars are based on 3 independent experiments.

129x67mm (300 x 300 DPI)

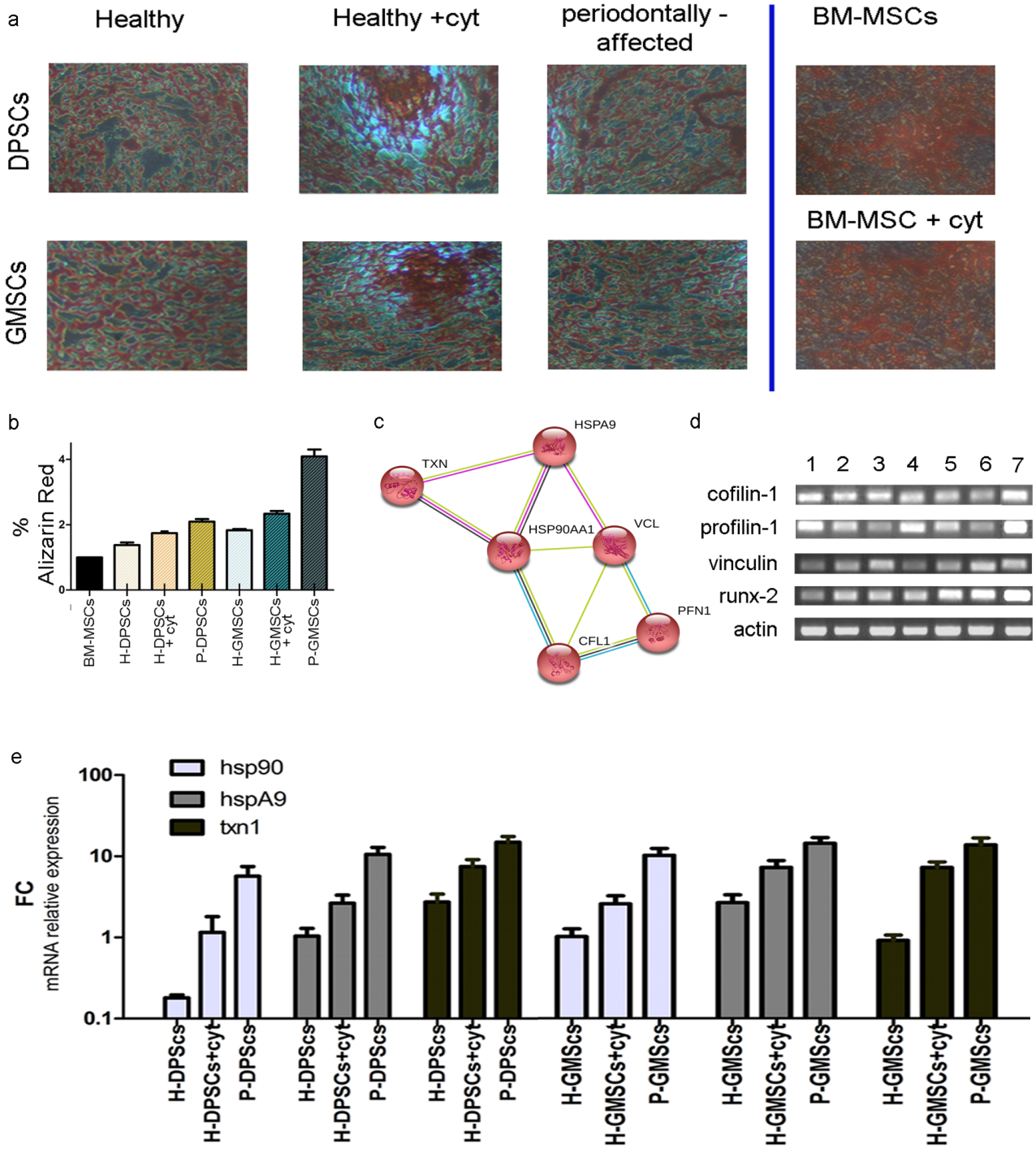

Fig.7 Bone in vitro formation: Inflammation – cytoskeleton modulation -osteogenesis: a) A representative image of Alizarin Red assay stained calcium deposits after 21 days of osteogenic differentiation of cultured H-DPSCs, H-GMSCs with or without cytokine treatment, P-DPSCs, P-GMSCs and BM-MSCs (control); b) the bar graph represents the quantitative analysis of the alizarin positive area performed with ImageJ software; c) the graph represents the interaction between anti-inflammatory and cytoskeleton-regulating proteins performed on http://string-db.org/ ; d) the gel lines represent the semi-quantitative PCR analysis for runx- 2, vinculin, profilin-1 and cofilin-1 (1: H-DPSCs; 2:H-DPSCs + cyt; 3: P-DPSCs; 4: H-GMSCs; 5: H-GMSCs + cyt; 6: P-GMSCs; 7: Positive control. cyt:20ng/ml IL1β + 40ng/ml TNF-α); e) the bar graph represents hsp90, hspA9 and txn1 real-time PCR analysis normalized to BM-MSCs control; (cyt: 20ng/ml IL-1β + 40ng/ml TNF-α). FC: fold change.

147x164mm (300 x 300 DPI)

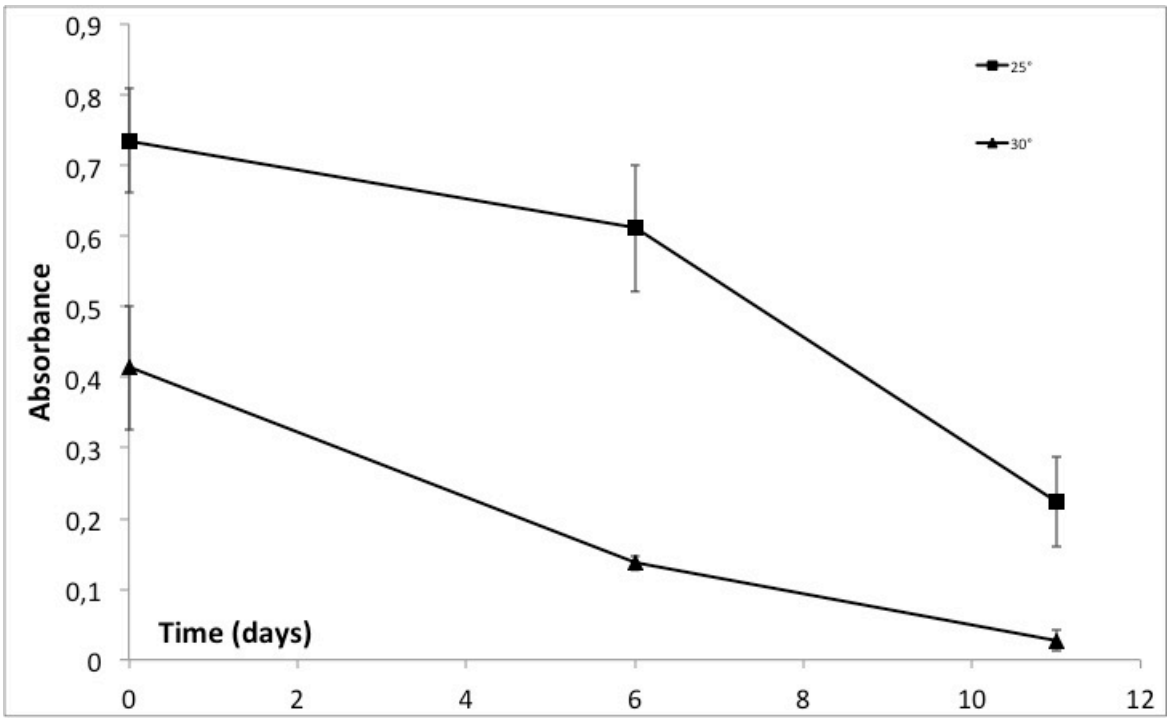

Fig. 8 CCK assay: Cell culture tests carried out on these supports showed a quick decrease of the number of viable P-GMSCs cells seeded on the surface of the scaffolds a and c during the examined culture period.

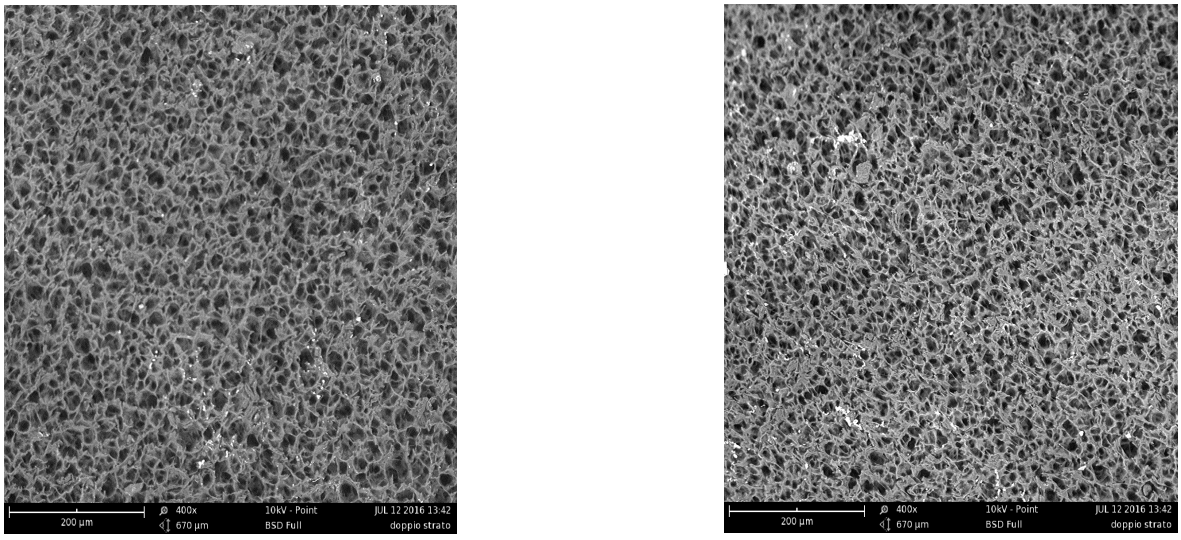

Fig. 9 SEM images of new scaffolds with smaller pores, (5/20 μm), 400x magnification

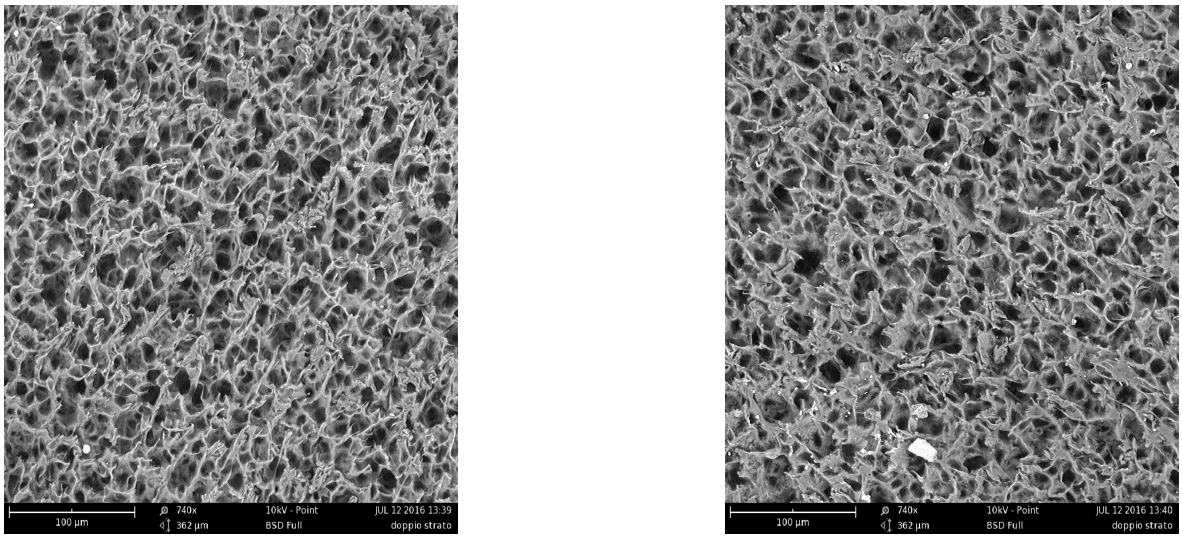

Fig. 10 SEM images of new scaffolds with smaller pores, (5/20 µm), 750x magnification

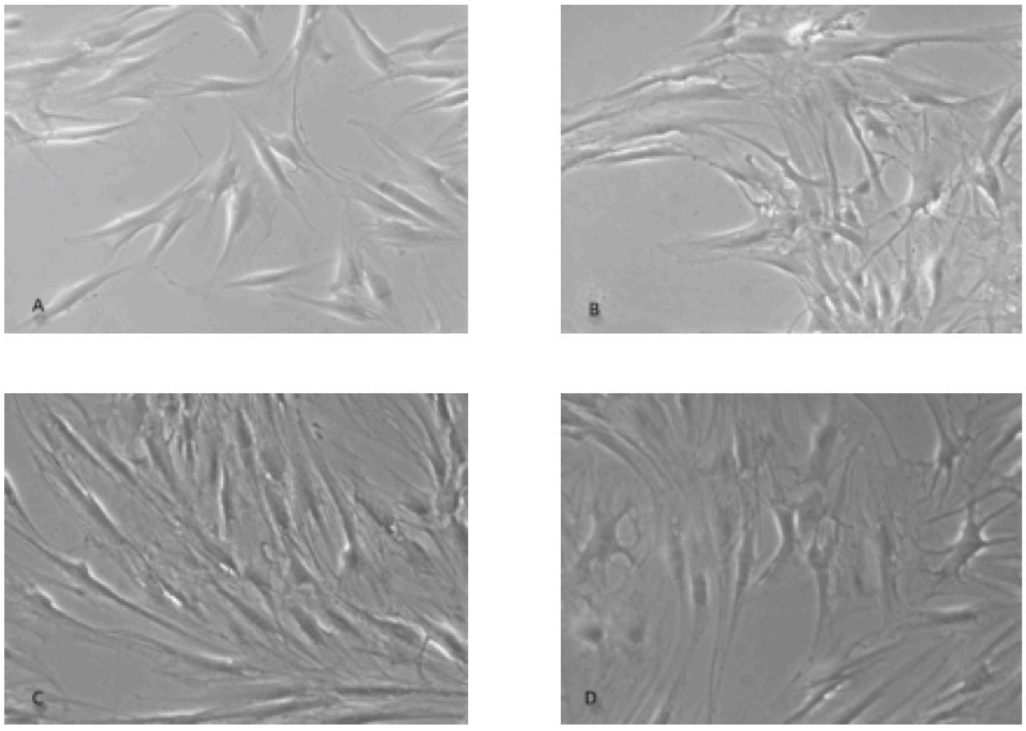

Fig. 11 P-GMSCs cell growth at different times. a) day 1;b) day 3; c) day 6; d) day 7.

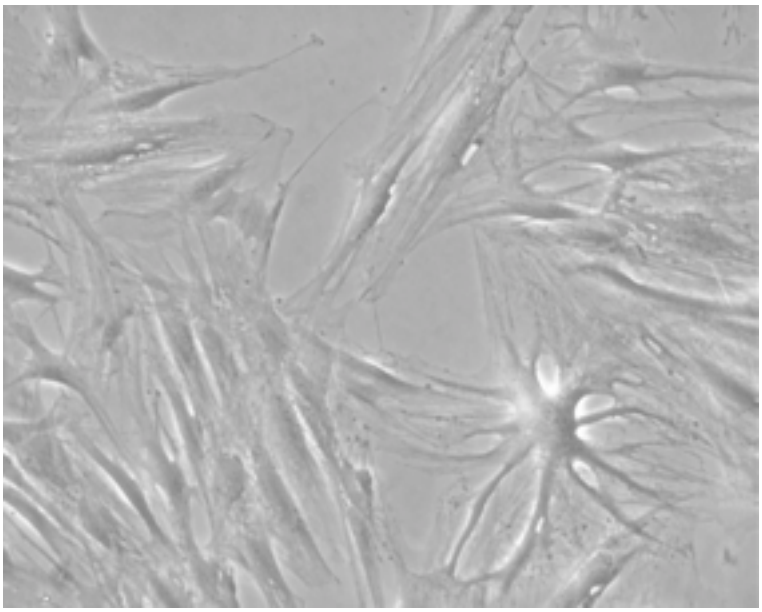

Fig. 12 P-GMSCs cell growth: similar astrocytes-like phenotype, day 6

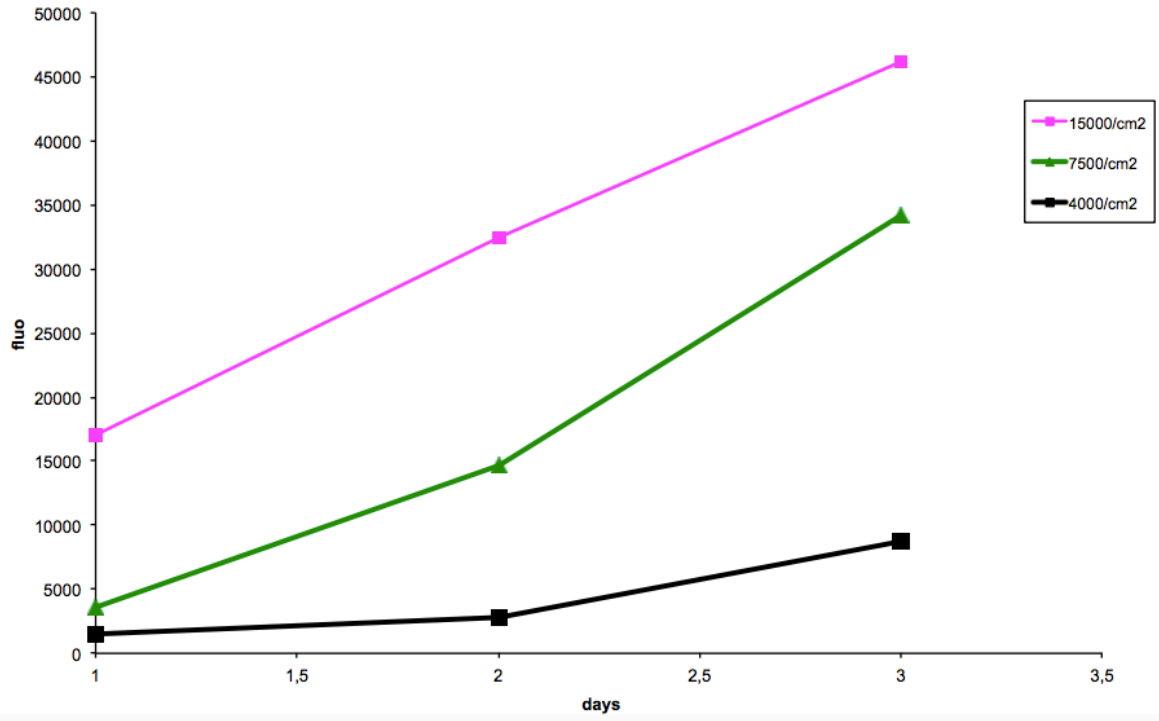

Fig. 13 P-GMSCs growth curve in 2D, plated at different cell concentrations, assessed by Alamar Blue assay

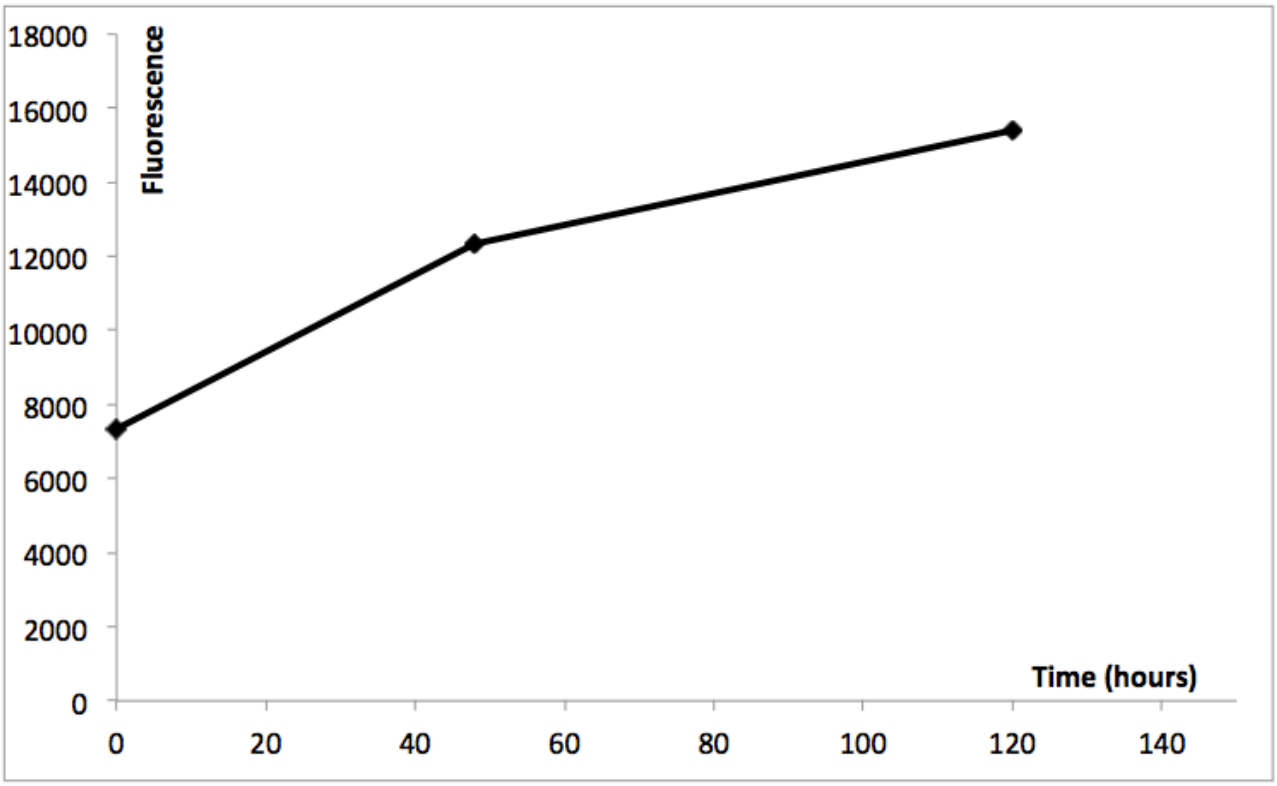

Fig 14 P-GMSCs Growth curve, on scaffold c, assessed by Alamar Blue assay

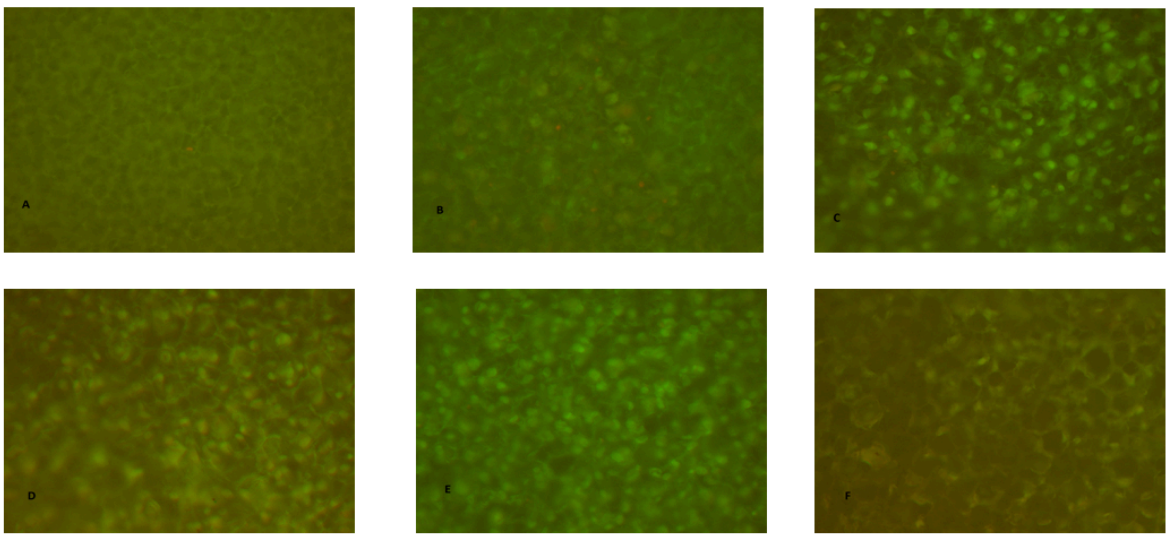

Fig. 15 AO/EB vitality assay of P-GMSCS on scaffold c

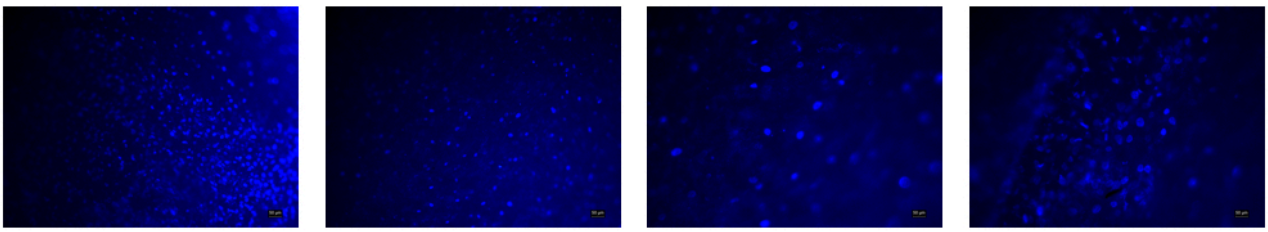

Fig. 16 DAPI assay of the P-GMSCs seeded on the scaffold c

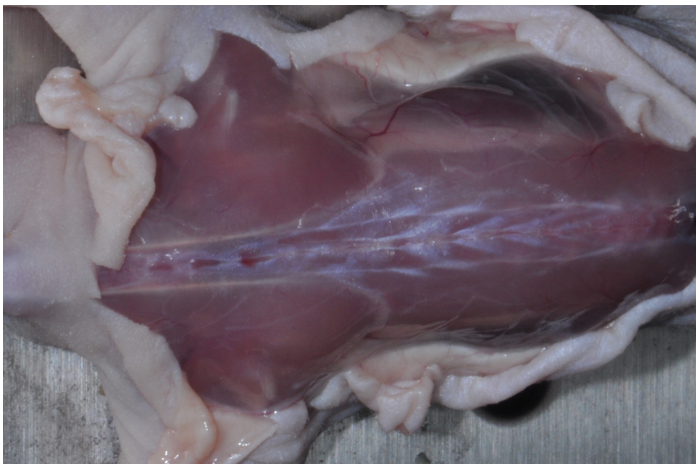

Fig. 17 In vivo study: in the picture the dorsal surface of one mouse of the first animal study group, no bone formation was observed

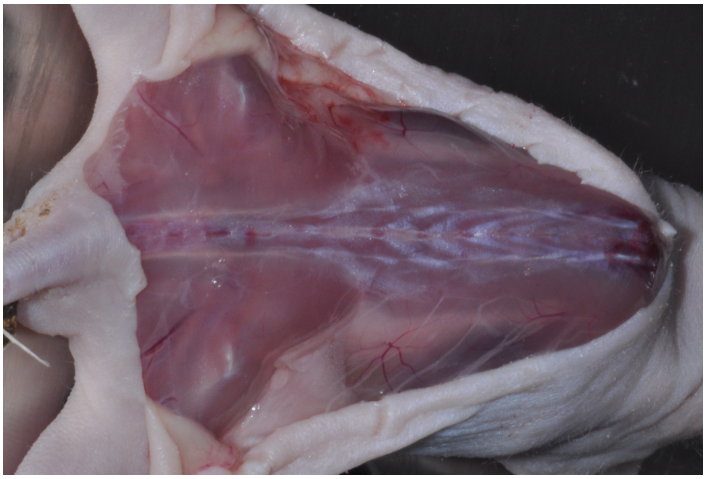

Fig. 18 In vivo study: in the picture the dorsal surface of one mouse of the second animal study group, no bone formation was observed

Bibliography

Bibliografy

1) Anusavice KJ. Standardizing failure, success, and survival decisions in clinical studies of ceramic and metal-ceramic fixed dental prostheses. Dent Mater. 2012 Jan;28(1):102-11.
2) Ye Y, Sun J. Simplified Complete Denture: A Systematic Review of the Literature. J Prosthodont. 2016 Feb 24. doi: 10.1111/jopr.12463.
3) Esposito M, Felice P, Worthington HV. Interventions for replacing missing teeth: augmentation procedures of the maxillary sinus. Cochrane Database Syst Rev. 2014 May 13;(5):CD008397.
4) Esposito M, Ardebili Y, Worthington HV. Interventions for replacing missing teeth: different types of dental implants. Cochrane Database Syst Rev. 2014 Jul 22;(7):CD003815.
5) Brånemark PI, Hansson BO, Adell R, Breine U, Lindström J, Hallén O, Ohman A. Osseointegrated implants in the treatment of the edentulous jaw. Experience from a 10-year period. Scand J Plast Reconstr Surg Suppl. 1977; 16:1-132.
6) Albrektsson T, Brånemark PI, Hansson HA, Lindström J. Osseointegrated titanium implants. Requirements for ensuring a long-lasting, direct bone-to-implant anchorage in man. Acta Orthop Scand. 1981;52(2):155-70.
7) Maiorana C, Farronato D, Pieroni S, Cicciu M, Andreoni D, Santoro F. A Four-Year Survival Rate Multicenter Prospective Clinical Study on 377 Implants: Correlations Between Implant Insertion Torque, Diameter, and Bone Quality. J Oral Implantol. 2015 Jun;41(3):e60-5.
8) Rodrigo D, Aracil L, Martin C, Sanz M. Diagnosis of implant stability and its impact on implant survival: a prospective case series study. Clin Oral Implants Res. 2010 Mar;21(3):255-61.
9) Trindade R, Albrektsson T, Wennerberg A. Current concepts for the biological basis of dental implants: foreign body equilibrium and osseointegration dynamics. Oral Maxillofac Surg Clin North Am. 2015 May;27(2):175-83.
10) Cawood JI, Howell RA. A classification of the edentulous jaws. Int J Oral Maxillofac Surg. 1988 Aug;17(4):232-6.
11) Lesolang RR, Motloba DP, Lalloo R. Patterns and reasons for tooth extraction at the Winterveldt Clinic: 1998-2002. SADJ. 2009 Jun;64(5):214-5, 218.
12) Tomasi C, Wennström JL, Berglundh T. Longevity of teeth and implants - systematic review. J Oral Rehabil. 2008 Jan;35 Suppl 1:23-32.
13) Becker BE, Becker W. Regeneration procedures: grafting materials, guided tissue regeneration, and growth factors. Curr Opin Dent. 1991 Feb;1(1):93-7.

14) Hämmerle CH, Jung RE, Feloutzis A. A systematic review of the survival of implants in bone sites augmented with barrier membranes (guided bone regeneration) in partially edentulous patients. J Clin Periodontol. 2002;29 Suppl 3:226-31; discussion 232-3
15) Retzepi M, Donos N. Guided Bone Regeneration: biological principle and therapeutic applications. Clin Oral Implants Res. 2010 Jun;21(6):567-76. doi: 10.1111/j.1600-0501.2010.01922.x.
16) Hermann JS, Buser D. Guided bone regeneration for dental implants. Curr Opin Periodontol. 1996;3:168-77. Review.
17) Esposito M, Grusovin MG, Felice P, Karatzopoulos G, Worthington HV, Coulthard P. Interventions for replacing missing teeth: horizontal and vertical bone augmentation techniques for dental implant treatment. Cochrane Database Syst Rev. 2009 Oct 7;(4):CD003607.
18) Kolk A, Handschel J, Drescher W, Rothamel D, Kloss F, Blessmann M, Heiland M, Wolff KD, Smeets R. Current trends and future perspectives of bone substitute materials - from space holders to innovative biomaterials. J Craniomaxillofac Surg. 2012 Dec;40(8):706-18.
19) Al-Nawas B, Schiegnitz E. Augmentation procedures using bone substitute materials or autogenous bone - a systematic review and meta-analysis. Eur J Oral Implantol. 2014 Summer;7 Suppl 2:S219-34.
20) Rakhmatia YD, Ayukawa Y, Furuhashi A, Koyano K. Current barrier membranes: titanium mesh and other membranes for guided bone regeneration in dental applications. J Prosthodont Res. 2013 Jan;57(1):3-14.
21) Burchardt H. Biology of bone transplantation. Orthop Clin North Am. 1987; 18:187-196.
22) Hallman M, Thor A. Bone substitutes and growth factors as an alternative/ complement to autogenous bone for grafting in implant dentistry. Periodontol 2000. 2008; 47:172-92.
23) Hing KA. Bone repair in the twenty-first century: biology, chemistry or engineering? Philos Transact A Math Phys Eng Sci. 2004; 362:2821-2850.
24) Caplan AI. Adult mesenchymal stem cells for tissue engineering versus regenerative medicine. J Cell Physiol. 2007;213(2):341-47.
25) Salgado AJ, Oliveira JM, Martins A et al. Tissue engineering and regenerative medicine: past, present, and future. Int Rev Neurobiol. 2013;108:1-33.
26) D'Aquino R, De Rosa A, Laino G, Caruso F et al. Human dental pulp stem cells: from biology to clinical applications. J Exp Zool B Mol Dev Evol. 2009;312B(5):408-15.
27) Liu J, Yu F, Sun Y, Jiang B et al. Concise reviews: Characteristics and potential applications of human dental tissue-derived mesenchymal stem cells. Stem Cells. 2015;33(3):627-38.
28) Nuti N, Corallo C, Chan BM, Ferrari M, Gerami-Naini B. Multipotent Differentiation of Human Dental Pulp Stem Cells: a Literature Review. Stem Cell Rev. 2016;12(5):511-23.
29) Graziano A, d'Aquino R, Laino G, Papaccio G. Dental pulp stem cells: a promising tool for bone regeneration. Stem Cell Rev. 2008 Spring;4(1):21-6. doi: 10.1007/s12015-008-9013-5. Review. Erratum in: Stem Cell Rev. 2008 Spring;4(1):65.

30) Lin NH, Gronthos S, Bartold PM. Stem cells and future periodontal regeneration. Periodontol 2000. 2009;51:239-51.

31) Hall PA, Watt FM. Stem cells: the generation and maintenance of cellular diversity. Development 1989; 106(4):619-33.

32) Hipp J, Atala A. Sources of stem cells for regenerative medicine. Stem Cell Rev. 2008 Spring;4(1):3-11.

33) Yu J, Wang Y, Deng Z, Tang L, Li Y, Shi J, Jin Y. Odontogenic capability: bone marrow stromal stem cells versus dental pulp stem cells. Biol Cell. 2007 Aug;99(8):465-74.

34) Alge DL, Zhou D, Adams LL, Wyss BK, Shadday MD, Woods EJ, Gabriel Chu TM, Goebel WS. Donor-matched comparison of dental pulp stem cells and bone marrow-derived mesenchymal stem cells in a rat model. J Tissue Eng Regen Med. 2010 Jan;4(1):73-81.

35) Gronthos S, Mankani M, Brahim J et al. Postnatal human dental pulp stem cells (DPSCs) in vitro and in vivo. Proc Natl Acad Sci USA 2000;97:13625-30.

36) Miura M, Gronthos S, Zhao M et al. SHED: stem cells from human exfoliated deciduous teeth. Proc Natl Acad Sci USA 2003;100:5807-12.

37) Seo B.M., Miura M., Gronthos S et al Investigation of multipotent postnatal stem cells from human periodontal ligament. Lancet 2004;364,149–55.

38) Sonoyama W, Liu Y, Yamaza T et al. Characterization of the apical papilla and its residing stem cells from human immature permanent teeth: a pilot study. J Endod 2008;34:166-71.

39) Zhang Q, Shi S, Liu Y et al. Mesenchymal stem cells derived from human gingiva are capable of immunomodulatory functions and ameliorate inflammation-related tissue destruction in experimental colitis. J Immunol 2009;183:7787-98.

40) Kawashima N. Characterisation of dental pulp stem cells: a new horizon for tissue regeneration? Arch Oral Biol. 2012 Nov;57(11):1439-58.

41) Laino G, Graziano A, d'Aquino R, Pirozzi G, Lanza V, Valiante S, De Rosa A, Naro F, Vivarelli E, Papaccio G. An approachable human adult stem cell source for hard-tissue engineering. J Cell Physiol. 2006 Mar;206(3):693-701.

42) de Mendonça Costa A, Bueno DF, Martins MT, Kerkis I, Kerkis A, Fanganiello RD, Cerruti H, Alonso N, Passos-Bueno MR. Reconstruction of large cranial defects in nonimmunosuppressed experimental design with human dental pulp stem cells. J Craniofac Surg. 2008 Jan;19(1):204-10.

43) d'Aquino R, De Rosa A, Lanza V, Tirino V, Laino L, Graziano A, Desiderio V, Laino G, Papaccio G. Human mandible bone defect repair by the grafting of dental pulp stem/progenitor cells and collagen sponge biocomplexes. Eur Cell Mater. 2009 Nov 12;18:75-83.

44) Huang AH, Chen YK, Chan AW, Shieh TY, Lin LM. Isolation and characterization of human dental pulp stem/stromal cells from nonextracted crown-fractured teeth requiring root canal therapy. J Endod. 2009;35(5):673-81.

45) Rajendran R, Gopal S, Masood H, Vivek P, Deb K. Regenerative potential of dental pulp mesenchymal stem cells harvested from high caries patient's teeth. J Stem Cells. 2013;8(1):25-41.

46) Wang Z, Pan J, Wright JT, Bencharit S, Zhang S, Everett ET, Teixeira FB, Preisser JS. Putative stem cells in human dental pulp with irreversible pulpitis: an exploratory study. J Endod. 2010;36(5):820-5.

47) Sun HH, Chen B, Zhu QL, Kong H, Li QH, Gao LN, Xiao M, Chen FM, Yu Q. Investigation of dental pulp stem cells isolated from discarded human teeth extracted due to aggressive periodontitis. Biomaterials. 2014;35(35):9459-72.

48) Palmer RM, Lubbock MJ. The soft connective tissues of the gingiva and periodontal ligament: are they unique? Oral Dis. 1995 Dec;1(4):230-7.

49) Zhang Q, Shi S, Liu Y, Uyanne J, Shi Y, Shi S, Le AD. Mesenchymal stem cells derived from human gingiva are capable of immunomodulatory functions and ameliorate inflammation-related tissue destruction in experimental colitis. J Immunol. 2009 Dec 15;183(12):7787-98. doi: 10.4049/jimmunol.0902318. Erratum in: J Immunol. 2010 Feb 1;184(3):1656.

50) Fournier BP, Ferre FC, Couty L, Lataillade JJ, Gourven M, Naveau A, Coulomb B, Lafont A, Gogly B. Multipotent progenitor cells in gingival connective tissue. Tissue Eng Part A. 2010 Sep;16(9):2891-9.

51) Tomar GB, Srivastava RK, Gupta N, Barhanpurkar AP, Pote ST, Jhaveri HM, Mishra GC, Wani MR. Human gingiva-derived mesenchymal stem cells are superior to bone marrow-derived mesenchymal stem cells for cell therapy in regenerative medicine. Biochem Biophys Res Commun. 2010 Mar 12;393(3):377-83.

52) Xu X, Chen C, Akiyama K, Chai Y, Le AD, Wang Z, Shi S. Gingivae contain neural-crest- and mesoderm-derived mesenchymal stem cells. J Dent Res. 2013 Sep;92(9):825-32.

53) Tang L, Li N, Xie H, Jin Y. Characterization of mesenchymal stem cells from human normal and hyperplastic gingiva. J Cell Physiol. 2011 Mar;226(3):832-42. doi: 10.1002/jcp.22405.

54) Fournier BP, Larjava H, Häkkinen L. Gingiva as a source of stem cells with therapeutic potential. Stem Cells Dev. 2013 Dec 15;22(24):3157-77.

55) Treves-Manusevitz S, Hoz L, Rachima H, Montoya G, Tzur E, Vardimon A, Narayanan AS, Amar S, Arzate H, Pitaru S. Stem cells of the lamina propria of human oral mucosa and gingiva develop into mineralized tissues in vivo. J Clin Periodontol. 2013 Jan;40(1):73-81.

56) Xu QC, Wang ZG, Ji QX, Yu XB, Xu XY, Yuan CQ, Deng J, Yang PS. Systemically transplanted human gingiva-derived mesenchymal stem cells contributing to bone tissue regeneration. Int J Clin Exp Pathol. 2014 Jul 15;7(8):4922-9.

57) Wang F, Yu M, Yan X, Wen Y, Zeng Q, Yue W, Yang P, Pei X. Gingiva-derived mesenchymal stem cell-mediated therapeutic approach for bone tissue regeneration. Stem Cells Dev. 2011 Dec;20(12):2093-102.

58) Li N, Liu N, Zhou J, Tang L, Ding B, Duan Y, Jin Y. Inflammatory environment induces gingival tissue-specific mesenchymal stem cells to differentiate towards a pro-fibrotic phenotype. Biol Cell. 2013 Jun;105(6):261-75.

59) Mravic M, Péault B, James AW. Current trends in bone tissue engineering. Biomed Res Int. 2014;2014:865270.

60) Oryan A, Alidadi S, Moshiri A, Maffulli N. Bone regenerative medicine: classic options, novel strategies, and future directions. J Orthop Surg Res. 2014 Mar 17;9(1):18.

61) Carfì-Pavia F, Turturici G, Geraci F, Brucato V, La Carrubba V, Luparello C, Sconzo G. Porous poly (L-lactic acid) scaffolds are optimal substrates for internal colonization by A6 mesoangioblasts and immunocytochemical analyses. J Biosci. 2009 Dec;34(6):873-9.

62) Schumann P, Tavassol F, Lindhorst D, Stuehmer C, Bormann KH, Kampmann A, Mülhaupt R, Laschke MW, Menger MD, Gellrich NC, Rücker M. Consequences of seeded cell type on vascularization of tissue engineering constructs in vivo. Microvasc Res. 2009 Sep;78(2):180-90.

63) Zou L, Luo Y, Chen M, Wang G, Ding M, Petersen CC, Kang R, Dagnaes-Hansen F, Zeng Y, Lv N, Ma Q, Le DQ, Besenbacher F, Bolund L, Jensen TG, Kjems J, Pu WT, Bünger C. A simple method for deriving functional MSCs and applied for osteogenesis in 3D scaffolds. Sci Rep. 2013;3:2243.

64) Carfì Pavia F, Palumbo FS, La Carrubba V, Bongiovì F, Brucato V, Pitarresi G, Giammona G. Modulation of physical and biological properties of a composite PLLA and polyaspartamide derivative obtained via thermally induced phase separation (TIPS) technique. Mater Sci Eng C Mater Biol Appl. 2016 Oct 1;67:561-9.

65) Peng F, Yu X, Wei M. In vitro cell performance on hydroxyapatite particles/poly(L-lactic acid) nanofibrous scaffolds with an excellent particle along nanofiber orientation. Acta Biomater. 2011 Jun;7(6):2585-92.

66) Hu J, Sun X, Ma H, Xie C, Chen YE, Ma PX. Porous nanofibrous PLLA scaffolds for vascular tissue engineering. Biomaterials. 2010 Nov;31(31):7971-7.

67) Park JE, Todo M. Development and characterization of reinforced poly(L-lactide) scaffolds for bone tissue engineering. J Mater Sci Mater Med. 2011 May;22(5):1171-82.

68) Pavia FC, La Carrubba V, Piccarolo S, Brucato V. Polymeric scaffolds prepared via thermally induced phase separation: tuning of structure and morphology. J Biomed Mater Res A. 2008 Aug;86(2):459-66.

69) Yang H, Gao LN, An Yet al. Comparison of mesenchymal stem cells derived from gingival tissue and periodontal ligament in different incubation conditions. Biomaterials 2013;34(29):7033-47.

70) Feng G, Zheng K, Song D et al. SIRT1 was involved in TNF-α-promoted osteogenic differentiation of human DPSCs through Wnt/β-catenin signal. In Vitro Cell Dev Biol Anim. 2016 Aug 16. DOI:10.1007/s11626-016-0070-9

71) Qin Z, Fang Z, Zhao L et al. High dose of TNF-α suppressed osteogenic differentiation of human dental pulp stem cells by activating the Wnt/β-catenin signaling. J Mol Histol. 2015;46(4-5):409-20.

72) Feng X, Feng G, Xing J et al. TNF-α triggers osteogenic differentiation of human dental pulp stem cells via the NF-κB signalling pathway. Cell Biol Int. 2013;37(12):1267-75.

73) Carrero R, Cerrada I, Lledó E et al. IL1β induces mesenchymal stem cells migration and leucocyte chemotaxis through NF-κB. Stem Cell Rev. 2012;8(3):905-16.

74) Cuerquis J, Romieu-Mourez R, François M, Routy JP, Young YK, Zhao J, Eliopoulos N. Human mesenchymal stromal cells transiently increase cytokine production by activated T cells before suppressing T-cell proliferation: effect of interferon-γ and tumor necrosis factor-α stimulation. Cytotherapy. 2014 Feb;16(2):191-202.

75) Fu X, Xiao J, Wei Y, Li S, Liu Y, Yin J, Sun K, Sun H, Wang H, Zhang Z, Zhang BT, Sheng C, Wang H, Hu P. Combination of inflammation-related cytokines promotes long-term muscle stem cell expansion. Cell Res. 2015 Jun;25(6):655-73. doi: 10.1038/cr.2015.58. Erratum in: Cell Res. 2015 Sep;25(9):1082-3.

76) Ennis WJ, Sui A, Bartholomew A. Stem Cells and Healing: Impact on Inflammation. Adv Wound Care (New Rochelle). 2013 Sep;2(7):369-378.

77) McBeath R, Pirone DM, Nelson CM, Bhadriraju K, Chen CS. Cell shape, cytoskeletal tension, and RhoA regulate stem cell lineage commitment. Dev Cell. 2004 Apr;6(4):483-95.

78) Yourek G, Hussain MA, Mao JJ. Cytoskeletal changes of mesenchymal stem cells during differentiation. ASAIO J. 2007;53(2):219-28.

79) Treiser MD, Yang EH, Gordonov S et al. Proc Natl Acad Cytoskeleton-based forecasting of stem cell lineage fates. Sci U S A. 2010;107(2):610-15.

80) Gao J, Fu S, Zeng Z, Li FF et al. Cyclic stretch promotes osteogenesis-related gene expression in osteoblast-like cells through a cofilin-associated mechanism Mol Med Rep. 2016; 14(1): 218–24.

81) Buer Sen, Zhihui Xie, Gunes Uzer et al.Stem Cells. Intranuclear Actin Regulates Osteogenesis Author manuscript. Stem Cells. 2015;33(10): 3065–76.

82) Ghosh M, Song X, Mouneimne G et al. Cofilin promotes actin polymerization and defines the direction of cell motility. Science. 2004;304(5671):743-6.

83) Chen L, Shi K, Frary CE et al. Inhibiting actin depolymerization enhances osteoblast differentiation and bone formation in human stromal stem cells. Stem Cell Res. 2015;15(2):281-9.

84) Kim HR, Graceffa P, Ferron F et al. Actin polymerization in differentiated vascular smooth muscle cells requires vasodilator-stimulated phosphoprotein. Am J Physiol Cell Physiol. 2010;298(3):C559-71.

85) Yun SP, Ryu JM, Jang MW, Han HJ. Interaction of profilin-1 and F-actin via a β-arrestin-1/JNK signaling pathway involved in prostaglandin E(2)-induced human mesenchymal stem cells migration and proliferation. J Cell Physiol. 2011;226(2):559-71.

86) Miyajima D1, Hayata T, Suzuki T et al. Profilin1 regulates sternum development and endochondral bone formation. J Biol Chem. 2012;287(40):33545-53.

87) Campos SB , Ashworth SL, Wean S et al. Cytokine-induced F-actin reorganization in endothelial cells involves RhoA activation. Am J Physiol Renal Physiol. 2009 ;296(3):F487-95.

88) Taiyab A, Rao ChM. HSP90 modulates actin dynamics: Inhibition of HSP90 leads to decreased cell motility and impairs invasion Biochim Biophys Acta. 2011;1813(1):213-21.

89) Imhoff BR1, Hansen JM. Differential redox potential profiles during adipogenesis and osteogenesis. Cell Mol Biol Lett. 2011;16(1):149-61.

Scientific Products (bound)

Publications discussed in this thesis:

"In vitro investigation on stem cells isolated from dental pulp and gingival tissues from periodontally compromised teeth." R. Mauceri, L. Tomasello, C. Giordano, G. Campisi, G. Pizzo. "I & J. Quintessenza Internazionale & Jomi", numero 4/2015 pagina 56;

"Mesenchymal stem cells derived from inflamed dental pulp and gingival tissue: a potential application for bone formation". L. Tomasello, R. Mauceri, A. Coppola, M. Pitrone, G. Pizzo, G. Campisi, G. Pizzolanti, C. Giordano. Stem Cells Translational Medicine (Submitted)

Publications not included in this thesis:

2014

"A simple protocol for medical-surgical tooth extractions in patients treated with bisphosphonates: our experience." ME Licata, A. Albanese, R. Mauceri, G. Giannatempo, L. Lo Russo, L. Lo Muzio. Minerva Stomatologica – Vol. 63 Suppl. 1 al N.4 (Aprile 2014), pagina 495;

"Segmental resection for the excision of two multicystic ameloblastoma". G. Capocasale, D. Perrone, R. Mauceri, B. Polizzi, L. Laino. Annali di Stomatologia No. 3 Vol. V - No. 2 - April/June 2014 – Quarterly, pagine 15-16;

"Evidence of field cancerization of oral squamous cell carcinoma: a case report". V. Panzarella, R. Mauceri, M. Dioguardi, G. Troiano, O. Di Fede. Annali di Stomatologia No. 3 Vol. V - No. 2 - April/June 2014 – Quarterly, pagina 34;

2015

"Paresthesia of the lip caused by a large osteoma of the mandible treated with a conservative approach: a case report." G. Giannatempo, G. Capocasale, N. Termine, R. Mauceri, L. Lo Russo, M. Giuliani. Minerva Stomatologica – Vol. 64 Suppl. I al N.2 (Aprile 2015), pagina 171;

"The surgical treatment of mandibular peripheral calcifying epithelial odontogenic tumour (pindborg tumor) with Er,Cr:YSGG laser: a case report." M. E. Licata, A. Albanese, G. Giannatempo, M. Dioguardi, R. Mauceri, G. Campisi. Minerva Stomatologica – Vol. 64 Suppl. I al N.2 (Aprile 2015), pagina 173.

"Painful oral aphthous-like lesions in patient with kidney cancer after target therapy and bisphosphonate administration: a case report of adverse drug reaction.". R. Mauceri, O. Di Fede, D. Perrone, G. Campisi, L. Laino. Minerva Stomatologica – Vol. 64 Suppl. I al N.2 (Aprile 2015), pagine 176-177;

"Triple simultaneus oral squamous cell carcinoma in a heavy smoker patient: a case report." Mauceri R., Panzarella V., Giuliani M., Lo Muzio L., Di Fede O. Annali di Stomatologia No. 3 Vol. VI Suppl. I - April/June 2015 – Quarterly, pagina 63 -

"Optical coherence tomography as a simple and non invasive tool for the diagnosis of oral disease: a case report." Capocasale G, Mauceri R, Troiano G, Lo Muzio L, Campisi G. Annali di Stomatologia No. 3 Vol. VI Suppl. I - April/June 2015 – Quarterly, pagina 52

"Use of porcine collagen matrix (Mucograft®) to promote the wound healing in the oral cavity". L. Laino, M. Giuliani, R. Mauceri, F. Giancola, G. Troiano. Annali di Stomatologia No. 3 Vol. VI Suppl. I - April/June 2015 – Quarterly, pagine 55-56

2016

"Dual localization of oral Kaposi's sarcoma in HIV-negative patient: a rare case report". G. Capocasale, R. Mauceri, De Lillo A, L. Lo Russo, F. Giancola, O. Di Fede. Minerva Stomatologica – volume 65 . SUPPL.1.No.3. JUNE 2016, pagine 195-196

"**Early onset ONJ in patient treated with denosumab and bevacizumab: case report**". F. Giancola, O. Di Fede, G. Giannatempo, L. Lo Muzio, R. Mauceri, G. Campisi. Minerva Stomatologica – volume 65 . SUPPL.1.No.3. JUNE 2016, pagine 201-202

"Healing evaluation by means of Optical Coherence Tomography of an extraction socket with L-PRF application in a patient at ONJ risk: a case report". R. Mauceri, G. Capocasale, G. Giannatempo, L. Lo Muzio, P. Tozzo, O. Di Fede. Minerva Stomatologica – volume 65 . SUPPL.1.No.3. JUNE 2016, pagina 207

"Oral lesions as primary manifestations of acute agranulocytosis related to metamizole: a case report". V. Panzarella, G. Campisi, L. Lo Russo, R. Mauceri, F. Giancola, O. Di Fede. Minerva Stomatologica – volume 65 . SUPPL.1.No.3. JUNE 2016, pagina 210-211

"Overexpression of Nicotinamide n-Methyl- transferase in HSC-2 OSCC cell line: effect on apoptosis and cell proliferation". G. Giannatempo, M. Mascitti, O. Di Fede, R. Mauceri, A. Santarelli, R. Seta, D. Sartini, R. Campagna, M. Emanuelli, L. Lo Muzio. Minerva Stomatologica – volume 65 . SUPPL.1.No.3. JUNE 2016, pagina 202

"Preliminary study about the efficiency of diode laser compared with retraction cords used for exposing the finishing lines of dental abutments before the optic impression". D. Melilli, R. Mauceri, N. Mauceri, ME Licata, G. Campisi, A. Albanese. Minerva Stomatologica – volume 65 . SUPPL.1.No.3. JUNE 2016, pagine 244 – 245

"Prevenzione e management odontoiatrico dei pazienti oncologici a rischio di osteonecrosi delle ossa mascellari da farmaci." G. Campisi; R. Mauceri; A. Bedogni; V.Fusco; O. Di Fede; V. Panzarella. Implants Italian Edition No. 2, 2016

"Prevenzione e management odontoiatrico dei pazienti oncologici a rischio di osteonecrosi delle ossa mascellari da farmaci." G. Campisi; R. Mauceri; A. Bedogni; V.Fusco; O. Di Fede; V. Panzarella. Dental Tribune Italian Edition No. 9, 2016 (ripubblicazione)

"L-PRF application in extraction sockets of bisphosphonate-treated patients: preliminary results." R. Mauceri, F. Giancola, V. Panzarella, P. Tozzo, G. Campisi, O. Di Fede. Oral Diseases – Volume 22- Suppl. 2 – September 2016, pagina 50

"Optical coherence tomography in oral medicine: preliminary in vivo study." G. Capocasale, V. Panzarella, R. Mauceri, V. Rodolico, G. Campisi, O. Di Fede. Oral Diseases – Volume 22- Suppl. 2 – September 2016, pagina 28

"L'odontoiatria a misura del paziente con patologia osteometabolica a rischio di osteonecrosi delle ossa mascellari da farmaci." G. Campisi; R. Mauceri; A. Bedogni; V.Fusco; O. Di Fede; V. Panzarella. Implant Tribune Italian Edition No. 4, 2016

"Surgical treatment for bisphosphonate-related osteonecrosis of the jaw by Er,Cr:YSGG laser and platelet-rich plasma in ten cancer patients: a longitudinal study." Licata M.E.; Mauceri R.; Albanese A.; Toia F.; Cumbo E.M.G.; Mazzola G.; Di Fede O.; Campisi G. Lasers in Medical Science (Submitted)

"The role of antibiotic prophylaxis in reducing bacterial contamination of autologous bone graft collected from implant site". R. Mauceri, G. Campisi, D. Matranga, L. Laino, M. Cicciù, E.M.G. Cumbo, G. Pizzo, D. Melilli. New Microbiologica (Submitted)